Cell

Tumor transcriptome-wide expression classifiers predict treatment sensitivity in advanced prostate cancers

Graphical abstract

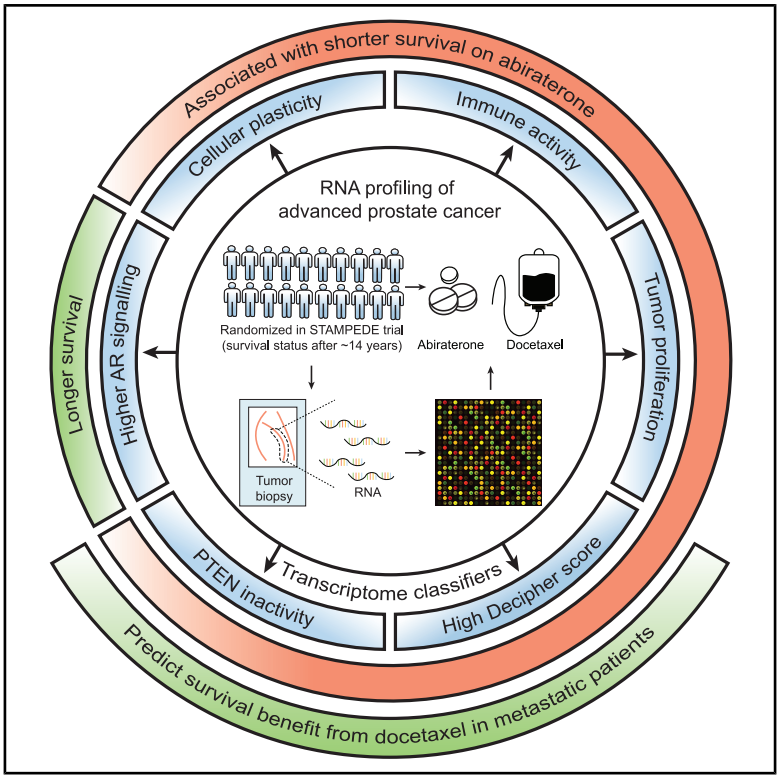

Authors

Emily Grist, Peter Dutey-Magni, Marina A. Parry, ..., Louise C. Brown, Nicholas D. James, Gerhardt Attard

Correspondence

g.attard@ucl.ac.uk

In brief

Large-scale analysis of phase 3 trial samples reveals novel biomarker-treatment pairings to guide therapy choices in metastatic prostate cancer.

Highlights

- Tumor RNA expression profiling in a platform trial with 14-year survival follow-up
- High proliferation or low androgen receptor activity are associated with shorter survival
- The Decipher classifier is prognostic and predicts docetaxel sensitivity
- PTEN-inactivated cancers have short survival but are docetaxel sensitive

Grist et al., 2025, Cell *188*, 5717–5734
October 2, 2025 © 2025 The Author(s). Published by Elsevier Inc.
https://doi.org/10.1016/j.cell.2025.07.042

CellPress

Cell

CellPress
OPEN ACCESS

Article

Tumor transcriptome-wide expression classifiers predict treatment sensitivity in advanced prostate cancers

Emily Grist,[1,22] Peter Dutey-Magni,[2,22] Marina A. Parry,[1,22] Larissa Mendes,[1,22] Ashwin Sachdeva,[3,4] James A. Proudfoot,[5] Anis A. Hamid,[6] Mazlina Ismail,[1] Sarah Howlett,[1] Stefanie Friedrich,[1] Lia DePaula Oliveira,[7] Laura Murphy,[2] Christopher Brawley,[2,23] Oluwademilade Dairo,[7] Sharanpreet Lall,[1] Yang Liu,[5] Daniel Wetterskog,[1] Anna Wingate,[1]

(Author list continued on next page)

[1]Cancer Institute, University College London, London, UK
[2]MRC Clinical Trials Unit at University College London, Institute of Clinical Trials and Methodology, University College London, London, UK
[3]The University of Manchester, Manchester, UK
[4]The Christie Hospital NHS Foundation Trust, Manchester, UK
[5]Veracyte, Inc, San Diego, CA, USA
[6]Memorial Sloan Kettering Cancer Center, New York, NY, USA
[7]Johns Hopkins School of Medicine, Baltimore, MD, USA
[8]Dana-Farber Cancer Institute, Boston, MA, USA
[9]Guy's and St Thomas' NHS Foundation Trust, London, UK
[10]University of Glasgow, Beatson West of Scotland Cancer Centre, Glasgow, UK
[11]St James's University Hospital, Leeds, UK
[12]Istituto Oncologico della Svizzera Italiana, EOC, Bellinzona, Switzerland
[13]The Royal Marsden NHS Foundation Trust and The Institute of Cancer Research, London, UK
[14]Prostate Cancer Research Center, Tampere University, Tampere, Finland
[15]Northwestern University Feinberg School of Medicine, Chicago, IL, USA
[16]University Hospitals Seidman Cancer Center, Case Western Reserve University, Cleveland, OH, USA
[17]University of South Australia, Adelaide, SA, Australia
[18]Barts Cancer Institute, Queen Mary University of London, London, UK
[19]University of California, San Francisco, San Francisco, CA, USA

(Affiliations continued on next page)

SUMMARY

Advanced prostate cancers respond to hormone therapy but outcomes vary and no predictive tests exist for informed treatment selection. To identify novel biomarker-treatment pairings, we examined associations between biological pathways and 14-year survival outcomes of patients randomized in practice-changing phase 3 trials (testing docetaxel or abiraterone). We included transcriptome-wide expression signatures and immunohistochemistry markers (Ki-67 and PTEN) on prostate tumors from 1,523 patients (832 metastatic). Tumor androgen receptor signaling is associated with longer survival, whereas increased proliferation predicted shorter survival. In a pre-specified analysis, the previously identified decipher RNA signature was both prognostic and predicted survival benefit from docetaxel for metastatic cancers (biomarker-docetaxel interaction $p = 0.039$). Additionally, transcriptome-based classification of PTEN inactivation identified tumors more likely to have PTEN protein loss ($p = 4 \times 10^{-37}$) and metabolically perturbed metastatic cancers that had shorter survival with hormone therapies ($p < 0.001$) but exhibited docetaxel sensitivity (biomarker-docetaxel interaction $p = 0.002$). Transcriptome classifiers predict docetaxel benefit and could be clinically implemented for improved patient management.

INTRODUCTION

Globally, prostate cancer accounts for a fifth of male cancer-related deaths, and the number of new cases is predicted to increase over the next two decades, exerting a major healthcare burden.[1] The majority of deaths occur in patients who present with advanced disease (metastatic or very high-risk localized).[2] Intensified anti-androgenic strategies combining androgen deprivation therapy (ADT) with an androgen receptor pathway inhibitor (ARPI), either abiraterone acetate and prednisone

This is an open access article under the CC BY license (http://creativecommons.org/licenses/by/4.0/).

CellPress
OPEN ACCESS

Cell
Article

Karolina Nowakowska,[1] Leila Zakka,[1] Claire L. Amos,[2] Nafisah B. Atako,[2,24] Victoria Wang,[8] Hannah L. Rush,[2,9] Robert J. Jones,[10] Hing Leung,[10] William R. Cross,[11] Silke Gillessen,[12] Chris C. Parker,[13] Teresa Marafioti,[1] Alfonso Urbanucci,[14] Matthew Fittall,[1] Edward M. Schaeffer,[15] Daniel E. Spratt,[16] David Waugh,[17] Thomas Powles,[18] Matthew R. Sydes,[2] Felix Y. Feng,[19,25] Daniel M. Berney,[18] Mahesh K.B. Parmar,[2] Noel W. Clarke,[3,4] Elai Davicioni,[5] Tamara L. Lotan,[7] Christopher J. Sweeney,[20] Louise C. Brown,[2] Nicholas D. James,[13] and Gerhardt Attard[1,21,26,*]

[20]South Australian Immunogenomics Cancer Institute, University of Adelaide, Adelaide, SA, Australia
[21]University College London Hospitals, London, UK
[22]These authors contributed equally
[23]Present address: Glaxo Smithkline Beecham, London, UK
[24]Present address: Gilead Sciences, London, UK
[25]Deceased
[26]Lead contact
*Correspondence: g.attard@ucl.ac.uk
https://doi.org/10.1016/j.cell.2025.07.042

(hereafter referred to as abiraterone) or an androgen receptor (AR) antagonist, improve survival when started as first-line treatment and are now the standard of care for this population.[3–7] For metastatic disease, the addition of docetaxel to ADT improves survival versus ADT alone, and some patients are now considered for combinations of ADT with docetaxel and an ARPI.[8–11] However, the physical and financial sequelae of treatment intensification are significant, so tests that improve risk stratification and predict treatment benefit could have a large healthcare impact.

One approach could be to stratify patients based on tumor molecular data. Loss of tumor suppressor genes such as *TP53* and phosphatase and tensin homolog (*PTEN*) associates with inferior outcomes.[12] By contrast, speckle-type POZ protein (*SPOP*) mutations may associate with better outcomes on hormone treatments.[13] The E26 transformation-specific (ETS) transcription factor ETS-related gene (ERG) is commonly overexpressed secondary to a gene fusion and may associate with prognosis.[14] Alterations of the *AR* gene can cause resistance to hormone therapies and commonly emerge after treatment, but these are rarely detected prior to treatment.[15,16]

However, despite a wealth of molecular data, a biomarker for selection of patients for combinations of hormone or cytotoxic therapy remains elusive. We reasoned that further progress requires integration of molecular analyses with well-curated clinical data from directly randomized patients at sufficient scale to detect statistically significant biomarker-treatment interactions. To achieve this, we used a clinical-grade microarray test optimized to generate transcriptome-wide expression profiles on diagnostic formalin-fixed, paraffin-embedded prostate tumors from patients participating in four multi-institutional phase 3 trials evaluating treatment intensification at the start of ADT.[11,17–19] We further integrated these data with analytically validated immunohistochemistry markers (Ki-67, PTEN).

We previously reported a first study on 160 patients randomized in the CHAARTED (chemohormonal therapy versus androgen ablation randomized trial for extensive disease in prostate cancer) trial to ADT or ADT and docetaxel.[20] We here report the next stage in which we analyzed tumors from men randomized to ADT, ADT with docetaxel, ADT with docetaxel and zoledronic acid, or ADT with abiraterone in three independently powered phase 3 trials conducted in the systemic therapy in advancing or metastatic prostate cancer: evaluation of drug efficacy (STAMPEDE) platform protocol.[6,17,18] These trials reported that combining ADT with (1) docetaxel improved survival for metastatic but not high-risk localized prostate cancer and (2) abiraterone improved survival when given continuously until progression for metastatic disease or for 2 years with prostate radiotherapy for very high-risk localized disease.[2,19] We have developed a framework to identify clinically relevant biological pathways to stratify patients or target therapeutically, establishing a resource of clinical-grade microarray expression data for linking diagnostic biopsy prostate tumor multi-gene transcriptome signatures with new 14-year overall survival data. We find for the first time that prostate tumor transcriptome signatures predict survival benefit from docetaxel, enabling better treatment selection for patients with advanced prostate cancer.

RESULTS

Characteristics of STAMPEDE abiraterone and docetaxel trials biomarker cohort

Between 5th October 2005 and 17th January 2014, the docetaxel trials and abiraterone trial conducted in the STAMPEDE platform protocol randomized 3,909 patients starting long-term ADT (2 years or longer), 3,879 of whom were randomized in the UK at 112 clinical sites and the remainder in Switzerland, where tissue collection was not allowed.[17–19] We retrieved routinely collected, formalin-fixed, paraffin-embedded tumors from 2,328 of 3,879 patients (60%). After central pathology review, prostate cancer samples from 1,699 patients had sufficient tumor purity and RNA yield for microarray hybridization, performed in a clinically accredited laboratory. Pan-transcriptome gene expression values from 1,523 patients with metastatic (n = 832) or non-metastatic (n = 691) prostate cancer passed quality control (Figures 1 and 2). Tissue for these cases was obtained from 1,427 diagnostic prostate core biopsies, 91 transurethral resections of the prostate, and five radical prostatectomies. Patients in the 1,523 biomarker cohort were randomized up to 31st March 2013 to either standard of care alone (control arm, n = 463) or with docetaxel (n = 233) or docetaxel and zoledronic acid (n = 199) or from 15th November 2011 to standard of care alone (n = 419) or with abiraterone (n = 375). During the period of overlapping recruitment, 15th November 2011 to 31st March 2013, 166 patients who received standard-of-care ADT were shared controls. There were no noticeable differences in clinical-pathological

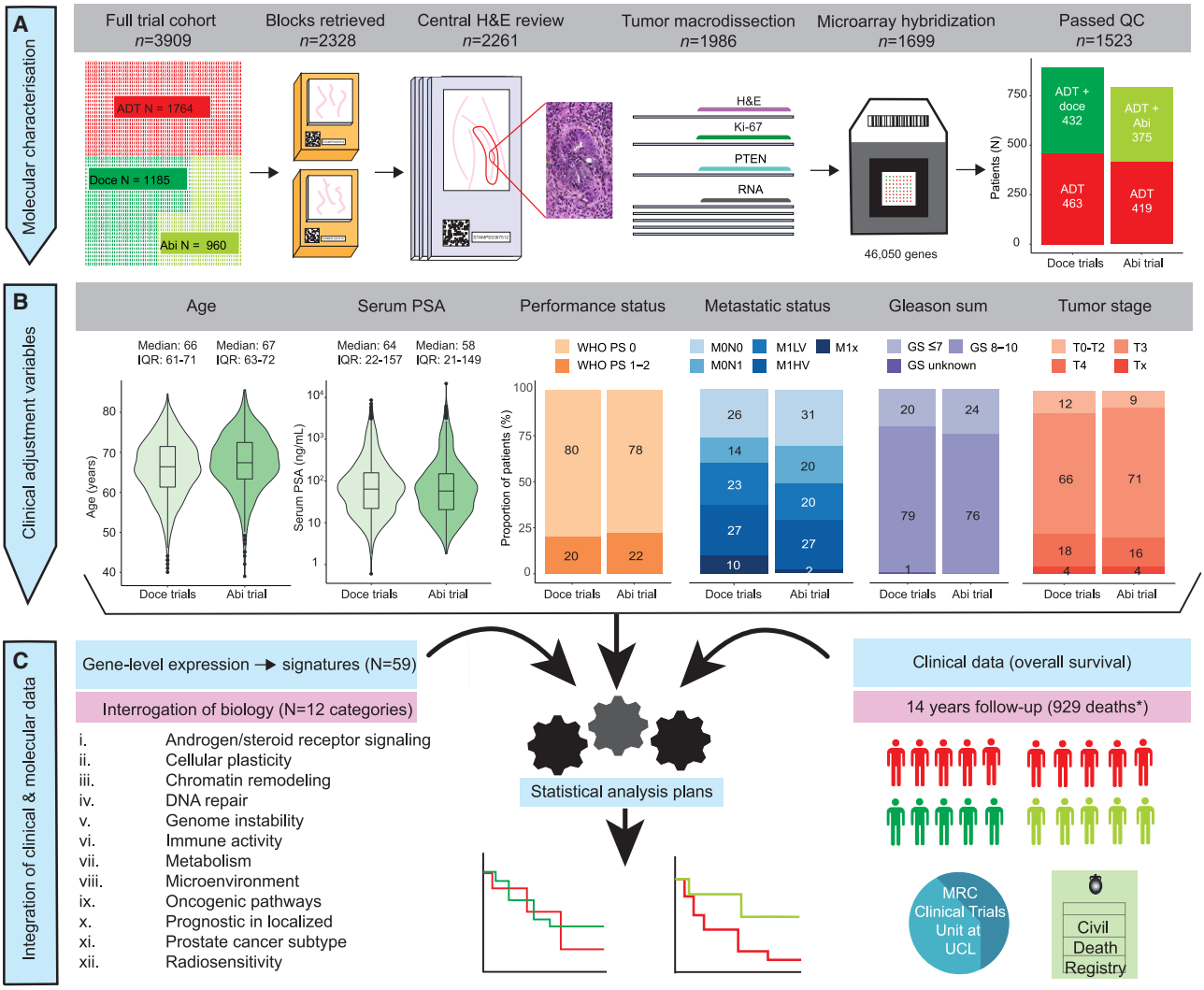

Figure 1. Cohort summary and study design

(A) Experimental and analytical workflow starting with the total number of patients randomized in docetaxel (doce) or abiraterone (abi) STAMPEDE trials, either to standard of care or combined with docetaxel or abiraterone. Scaled to show shared control patients. Ending with the final biomarker cohort, the number of patients retained at each step is shown.

(B) Box-violin plots and stacked bars show the range or distribution of baseline clinical variables that were adjusted for in multivariable models, relating to Table S1.

(C) Overall summary of multivariable models constructed to integrate transcriptome signatures, clinical variables, treatment allocation, and long-term survival data, relating to Tables S1, S2, S3, and S4. *155 deaths reported among the shared control patients; IQR, interquartile range; QC, quality control; M0N0, non-metastatic node negative; M0N1, non-metastatic with local lymph node involvement; M1LV, metastatic low volume; M1HV, metastatic high volume; M1x, metastatic, disease volume unknown.

characteristics between the full trial and biomarker cohorts, which is expected given the large number of patients included (Table S1). Radical radiotherapy was planned for 67% of high-risk localized patients in the docetaxel trials and 84% in the abiraterone trial (none of the patients with metastatic disease). The time from biopsy to randomization for patients starting their primary treatment for synchronous metastatic or high-risk localized disease (n = 1,484, 97%) was a median of 77 days (interquartile range [IQR] = 57–98, Table S2). Of the biomarker cohort (as of February 2024), 638 patients (71%) randomized in the docetaxel trials and 446 (56%) in the abiraterone trial were reported to have died (Table S3).

Landscape of tumor transcriptome-wide expression signatures in advanced prostate cancer

We reviewed prior publications and identified transcriptome-wide expression signatures generated in prostate cancer or other cancer types. These were pre-computed (using the code or gene data from the original publications) and optimized on 80,071 prostate cancers. We then used normalized pan-transcriptome

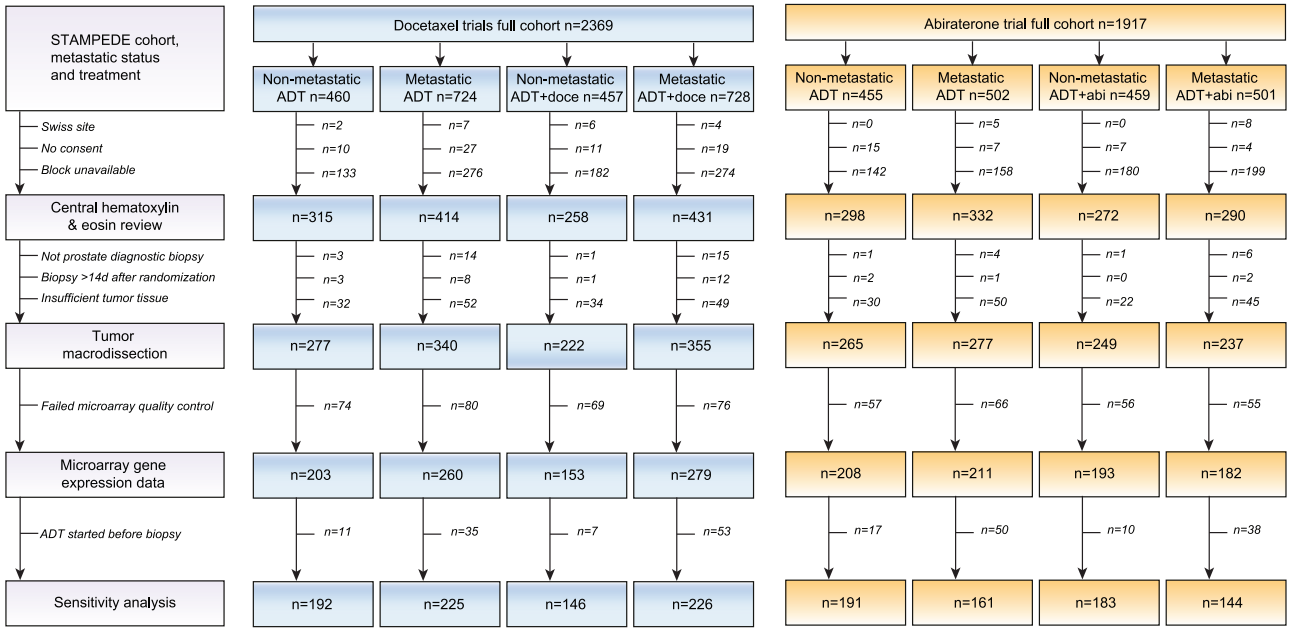

Figure 2. Sample flow diagram

Sample flow diagram starting from the number of patients randomized in the full trial cohorts and ending with numbers of quality-pass expression profiles in the docetaxel and abiraterone STAMPEDE trials (n = 166 patients randomized to the control arm shared across the abiraterone and docetaxel trials).

gene values to generate signature scores for every tumor in the biomarker cohort. We restricted our primary analysis to <60 signatures to reduce the risk of false discoveries from multiple testing. Other signatures can be evaluated in the future in exploratory studies to test biological hypotheses of interest to the research community. In addition to the four signatures we had tested in the CHAARTED trial,[20] we expanded our analyses to 59 signatures that summarized expression data representative of biological processes we hypothesized are relevant to prostate cancer (Figure 3; Table S4). Twenty-six were developed in prostate cancer, and 33 were developed using other tumor types (pan-cancer or exclusively bladder, breast, gastric, or renal cancer or melanoma).

Two basal-luminal subtyping signatures were categorical: we used both the prediction analysis of microarray 50 signature[21] (PAM50, developed in breast cancer) and a bespoke prostate subtyping classifier (PSC).[22] PAM50 luminal A patients have excellent post-prostatectomy outcomes,[23] and consistent with this, 2% of tumors from STAMPEDE patients were classified as luminal A compared with 43% in low-risk, localized disease (chi-squared test of independence $p < 0.001$, Figures S1A and S1B). The ERG signature was generated as a continuous score but, given the expected bimodal distribution related to fusion-driven ERG overexpression, was used as a categorical signature[24] (Figures S1C–S1E).

The other 56 signatures had continuous scores. We tested the correlation of each continuous signature with every other signature (Figure 3; Table S5). Key oncogenic pathways (TP53 and PTEN, commonly aberrant in prostate cancer) were represented by >1 signature developed in different datasets (PTEN loss[25,26] n = 2, Spearman rho = 0.51 and TP53 loss[27,28] n = 2, Spearman rho = 0.42). Within the biological category steroid receptor signaling,[29–34] the AR signaling signatures (with gene overlap) were mostly correlated (for example, AR_Kumar and AR-A_Spratt Spearman rho = 0.82), and biologically plausibly, these signatures were anti-correlated with signatures associated with neuroendocrine disease[33–38] in the cellular plasticity category (AR-A_Spratt and NE_Alshalalfa, Spearman rho = −0.65). AR signaling was also anti-correlated with basal subtyping (Spearman rho < −0.70), which is consistent with prior reports that basal subtypes had low expression of luminal markers.[39] In patients with non-metastatic disease, we noted a correlation between tumor AR signaling and pre-ADT serum PSA (PSA and AR-A_Spratt,[29] Spearman rho = 0.34; PSA and AR_HM,[33] Spearman rho = 0.31, Figure S1F). Although the correlation is relatively weak, we posit that this is notable for a comparison between a tumor biopsy and a blood sample. This result could suggest that although serum PSA is routinely used as an indicator of disease volume and risk of spread, it may also in part capture tumor AR signaling.

We used STAMPEDE tumor transcriptome-wide data to identify genes that showed a correlation with each continuous signature and then performed pathway enrichment analysis on correlated genes (54 of 56 continuous signatures had a sufficient number of correlated genes for pathway enrichment, Table S6). We identified that 35% (19 of 54) of continuous signatures had a biological consequence that enriched for the cell-cycle pathway (as annotated in the Kyoto Encyclopedia of Genes and Genomes [KEGG], q value < 1×10^{-5}, Figure 3), and these signatures often also had enrichment for DNA replication, DNA repair pathways, and p53 signaling (Table S6). Among these "proliferative" signatures we noted signatures developed in various ways, including

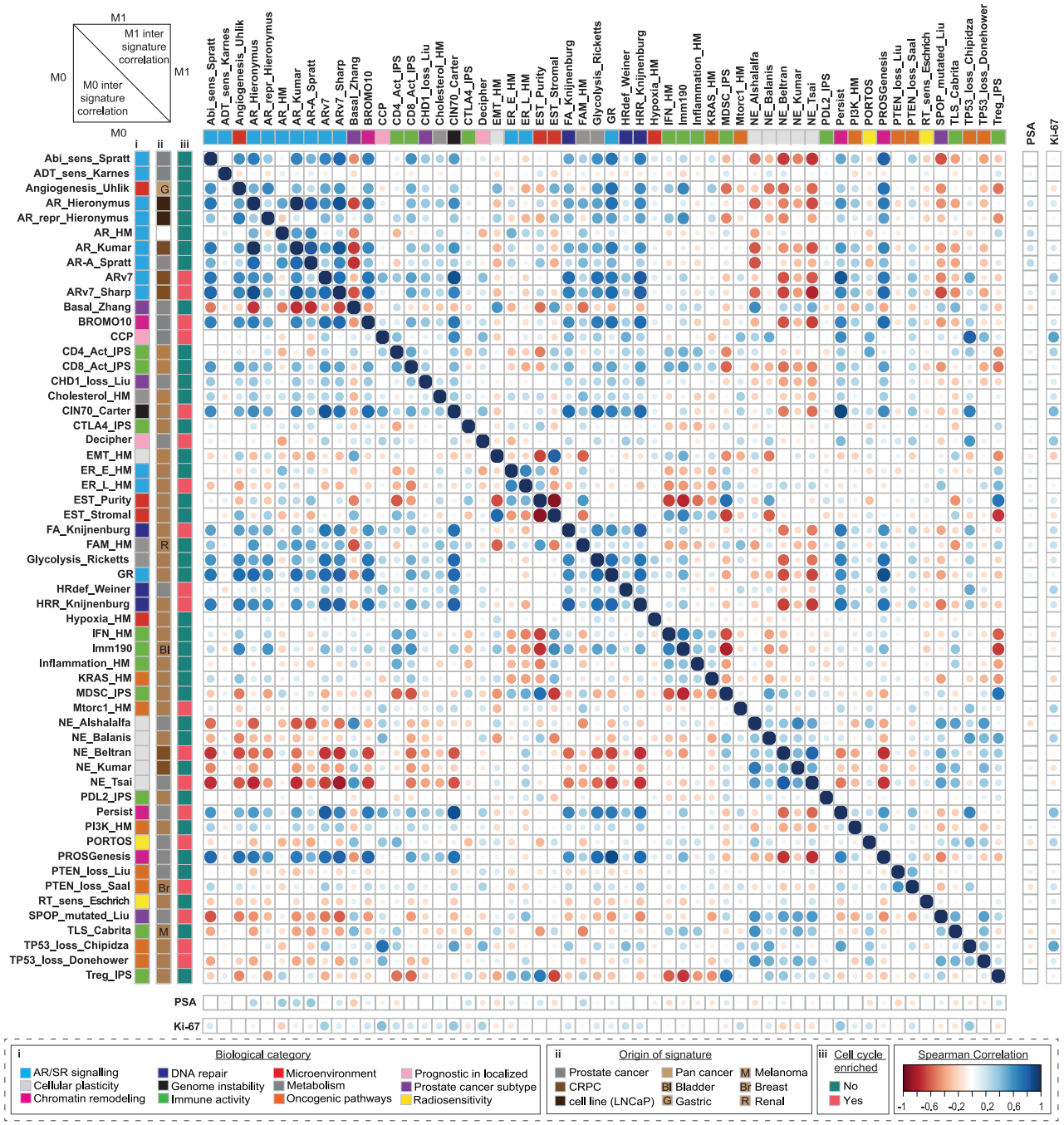

Figure 3. Landscape of transcriptome-wide expression signatures in advanced prostate cancer

Matrix of pairwise Spearman rho correlation values of 56 (continuous) transcriptome signature scores (see Table S4) ordered alphabetically and separated for tumors from patients with non-metastatic (M0) disease in the bottom-left triangle and metastatic (M1) disease in the top-right triangle, relating to Table S5. Correlations with Ki-67 immunohistochemistry and serum PSA are included in separate rows and columns. The size of the circle represents the magnitude of correlation, and the color and intensity represent the direction and magnitude of correlation. Vertical columns adjacent to signature names denote (i) biological category, (ii) cancer type in which the signature was developed, and (iii) whether the signature showed enrichment with the KEGG cell-cycle pathway (q value $< 1 \times 10^{-5}$), relating to Table S6. SR, steroid receptor; CRPC, castration-resistant prostate cancer.

See also Figure S1.

signatures commercially available for assessing prognosis in localized disease Decipher[40] and Cell-Cycle Proliferation (CCP)[41] and signatures developed to predict biological processes, such as TP53 loss, genome instability, or DNA repair (TP53_loss_Chipidza,[27] CIN70_Carter,[42] and HRdef_Weiner,[43] respectively). As an exemplar of transcriptome signatures capturing biological processes shared across cancer types, CIN70_Carter was developed as a pan-cancer indicator of chromosomal instability but with no prostate cancer samples in the discovery set.[42] As a means of orthogonal validation of "proliferative" signatures, we evaluated the proliferative index Ki-67 immunohistochemically on an adjacent slide and found this correlated most strongly (Spearman rho = 0.50) with the CCP signature, trained to predict biochemical failure in patients who had a radical prostatectomy and time to death from prostate cancer in a transurethral resection of the prostate cohort.[41] We also observed a consistent but less strong correlation (Spearman rho = 0.38) for Ki-67 immunohistochemistry and the Decipher signature, trained in a high-risk cohort to predict time to development of metastases.[40] Consistent with this, Decipher had a moderate correlation with CCP[41] (Spearman rho = 0.40). We were interested in differences in the distribution of proliferation across disease states. CCP scores and Ki-67 immunohistochemistry showed a progressively higher distribution, albeit not large, with increasing STAMPEDE tumor metastatic burden (Figures S1G and S1H). By contrast, there was no difference in Decipher score distribution between non-metastatic, node-positive, and metastatic tumors of low or high volume ($p = 0.307$), but we confirmed Decipher scores were significantly higher with increasing risk in localized disease (non-metastatic, node-negative versus node-positive STAMPEDE tumors F test [two-way ANOVA], $p = 2.71 \times 10^{-11}$, Figures S1I and S1J).

Tumor transcriptome-wide expression signatures are biologically and clinically informative

We performed multivariable-adjusted analysis (refer to STAR Methods) to test associations with survival of transcriptome signatures (44 continuous, 12 continuous and categorical, and 3 categorical) and Ki-67 immunohistochemistry (both continuous and categorical) split by metastatic status and adjusted for treatment allocation. Statistical significance of the effect, irrespective of its direction, was tested using partial likelihood ratio tests (Bonferroni corrected p value $< 8.3 \times 10^{-4}$). Sixteen of 59 signatures (27%) had statistically significant associations with survival in non-metastatic and/or metastatic disease (Figure 4A for continuous signatures, Figure 4B for categorical signatures, and Table S7 for all signatures and sensitivity analyses).

The three signatures that showed consistent associations with worse survival in both disease states had shown enrichment for the cellcycle pathway, namely CCP,[41] TP53 loss (TP53_loss_Chipidza),[27] and Decipher.[40] Despite relatively limited overlap of genes across all three signatures and differences in the score distributions (Figure 4C), the prognostic associations were too similar to compare individually. Based on our previous analyses of the CHAARTED trial,[20] Decipher had been selected (with AR-A_Spratt, PAM50, and PSC) prior to linking with clinical data for primary prognostic analyses. In metastatic disease, a one standard deviation increase in Decipher score associated with an increase in hazard of death of 26% (standardized hazard ratio [sdHR] 1.26, 95% confidence intervals [CIs] 1.15–1.38, $p = 2 \times 10^{-7}$, Figure 4A). Overall, the Decipher score as a continuous variable (score range: 0.07–1.0) was strongly associated with overall survival in the docetaxel and abiraterone trials, with every 0.1 increment associating in both trials combined with an increase in hazard of death of 11% (HR 1.11, 95% CI 1.06–1.15, $p = 2 \times 10^{-7}$) in patients with metastatic disease and 14% (HR 1.14, 95% CI 1.08–1.20, $p = 4 \times 10^{-6}$) in non-metastatic disease (Table S7). Given the overlapping biological processes tested for by the CCP signature and Ki-67 immunohistochemistry, we a priori planned to formally test for differences in prognostic effect between these orthogonal approaches in the subset with Ki-67 immunohistochemistry ($n = 1{,}203$). We found equivalent goodness-of-fit in a partial deviance test in metastatic ($\chi^2_{(df = 1)} = 0.05$, $p = 0.815$) and non-metastatic ($\chi^2_{(df = 1)} = 2.35$, $p = 0.125$) disease. Additional signatures that showed enrichment for the cell-cycle pathway showed different magnitudes of worse prognoses across metastatic disease states (Table S7). These included homologous recombination deficiency (HRdef_Weiner,[43] sdHR 1.16, 95% CI 1.08–1.25, $p = 1 \times 10^{-4}$), chromatin remodeling (persist,[44] sdHR 1.18, 95% CI 1.09–1.27, $p = 2 \times 10^{-5}$), and chromosomal instability (CIN70_Carter,[42] sdHR 1.15, 95% CI 1.07–1.23, $p = 4 \times 10^{-4}$), which were associated with shorter survival in metastatic disease, while postoperative radiation therapy outcomes score (PORTOS),[45] a signature that identifies poor prognosis localized cancers with greater radiation sensitivity, was associated with shorter survival in non-metastatic disease (sdHR 1.27, 95% CI 1.14–1.43, $p = 4 \times 10^{-5}$).

We intentionally included several signatures representative of androgen or steroid receptor signaling and pre-specified AR-A_Spratt[29] as a primary signature of interest in the abiraterone trials. These signatures showed enrichment for pathways associated with endocytosis and protein processing in the endoplasmic reticulum (Table S6). High AR-A_Spratt activity was associated with longer survival than low activity in both metastatic (HR 0.78, 95% CI 0.66–0.92) and non-metastatic (HR 0.58, 95% CI 0.46–0.74, Table S7) disease. Across other signatures in the same class, there was a consistent association with longer survival in both non-metastatic (AR_Hieronymus[32] $p = 1 \times 10^{-4}$, AR_Kumar[34] $p = 2 \times 10^{-5}$, and AR_HM[33] $p = 9 \times 10^{-7}$) and metastatic (ER_E_HM[33] $p = 1 \times 10^{-4}$ and AR_HM[33] $p = 4 \times 10^{-5}$) disease (Figure 4D; Table S7). Prior ADT reduces AR signaling scores, so we confirmed the association was consistent across all tumors in sensitivity analyses that excluded patients in whom ADT was initiated prior to biopsy (198 [13%] patients, median interval between biopsy and ADT start: 14 days, IQR = 6–27; 6% of non-metastatic [$n = 39$], 8% of low-volume metastatic [$n = 27$], 28% of high-volume metastatic [$n = 121$], and 22% of metastatic volume unknown [$n = 11$], Figure 4D; Table S7). Conversely, signatures of neuroendocrine disease (NE_Alshalalfa,[35] sdHR 1.37, 95% CI 1.23–1.53, $p = 4 \times 10^{-7}$) and basal cell-of-origin gene expression (Basal_Zhang[46] sdHR 1.37, 95% CI 1.22–1.55, $p = 3 \times 10^{-7}$) that captured states of low AR signaling were associated with shorter survival in non-metastatic disease (Table S7). Although categorical luminal-basal phenotyping (PAM50 and PSC, our two other primary prognostic signatures), previously reported as prognostic in localized cohorts,[22,23] did not show

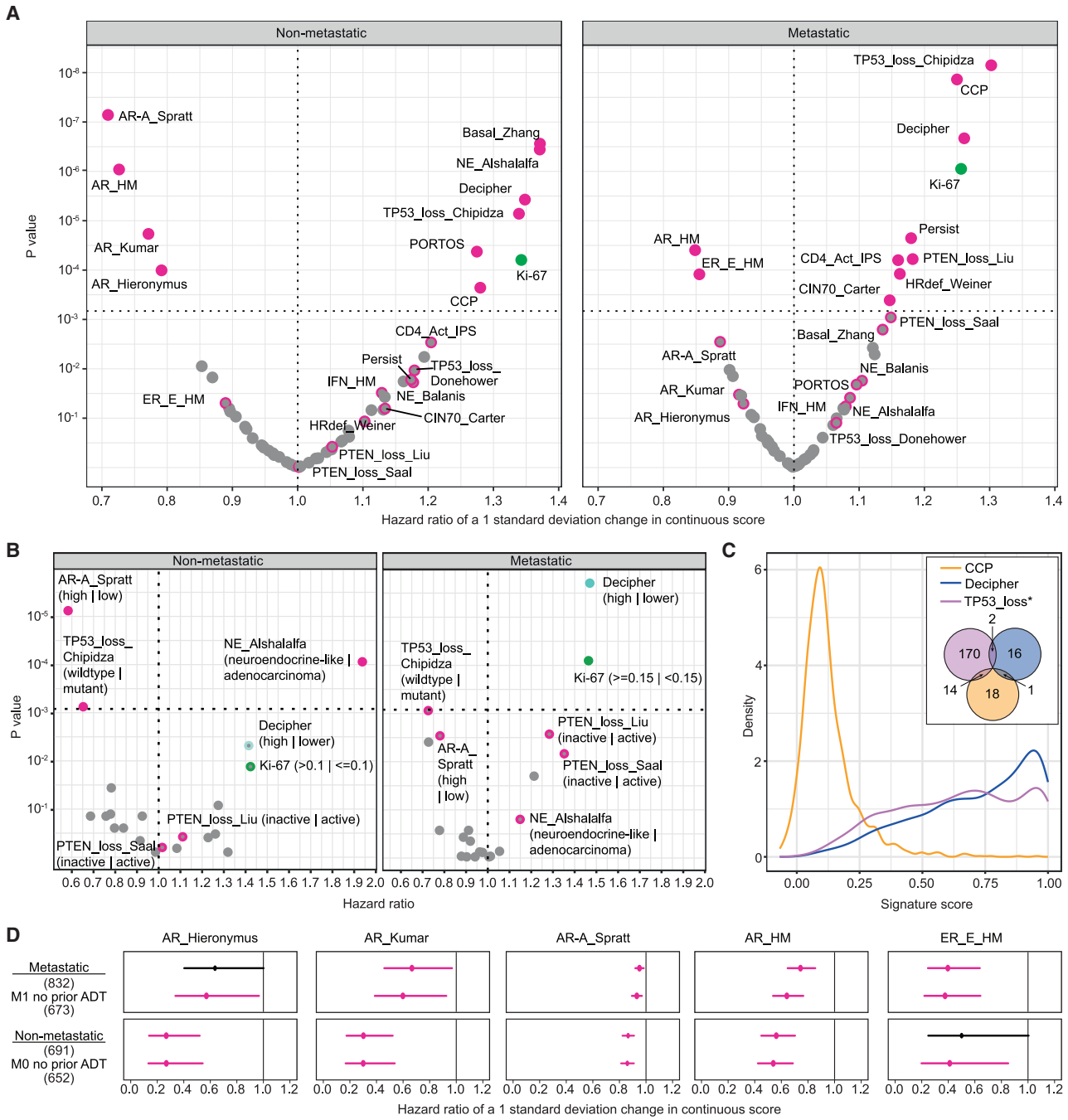

Figure 4. Transcriptome signatures are clinically and biologically informative

(A and B) Scatterplot of HR and *p* values from survival testing of (A) 56 signatures with continuous scores and Ki-67 immunohistochemistry and (B) 15 classifiers with categorical scores and Ki-67 immunohistochemistry, adjusted for clinical and pathological variables and treatment allocation, split by non-metastatic or metastatic disease, relating to Table S7. Dots that meet pre-specified levels for statistical significance ($p < 8.3 \times 10^{-4}$, marked by dashed lines) are colored pink, and Ki-67 immunohistochemistry is colored green. Other signatures or classifiers are gray with outline circles if statistically significant in the other metastatic state and/or in one trial arm. Classifiers are labeled in brackets with the effect corresponding to the HR, followed by the reference category.

(C) Density plot of signature score distributions for Decipher, CCP, and TP53_loss_Chipidza. Inset Venn diagram showing gene overlap across Decipher, CCP, and TP53_loss_Chipidza(*) signatures, relating to Table S4.

(D) Forest plots showing HRs and 95% CIs (whiskers) for survival estimates split by metastatic status for statistically significant AR/SR signaling pathway signatures, relating to Table S7. Estimates are also included after removal of patients who had received ADT at the time of biopsy. Pink lines represent statistical significance below the threshold of *p* value < 0.05.

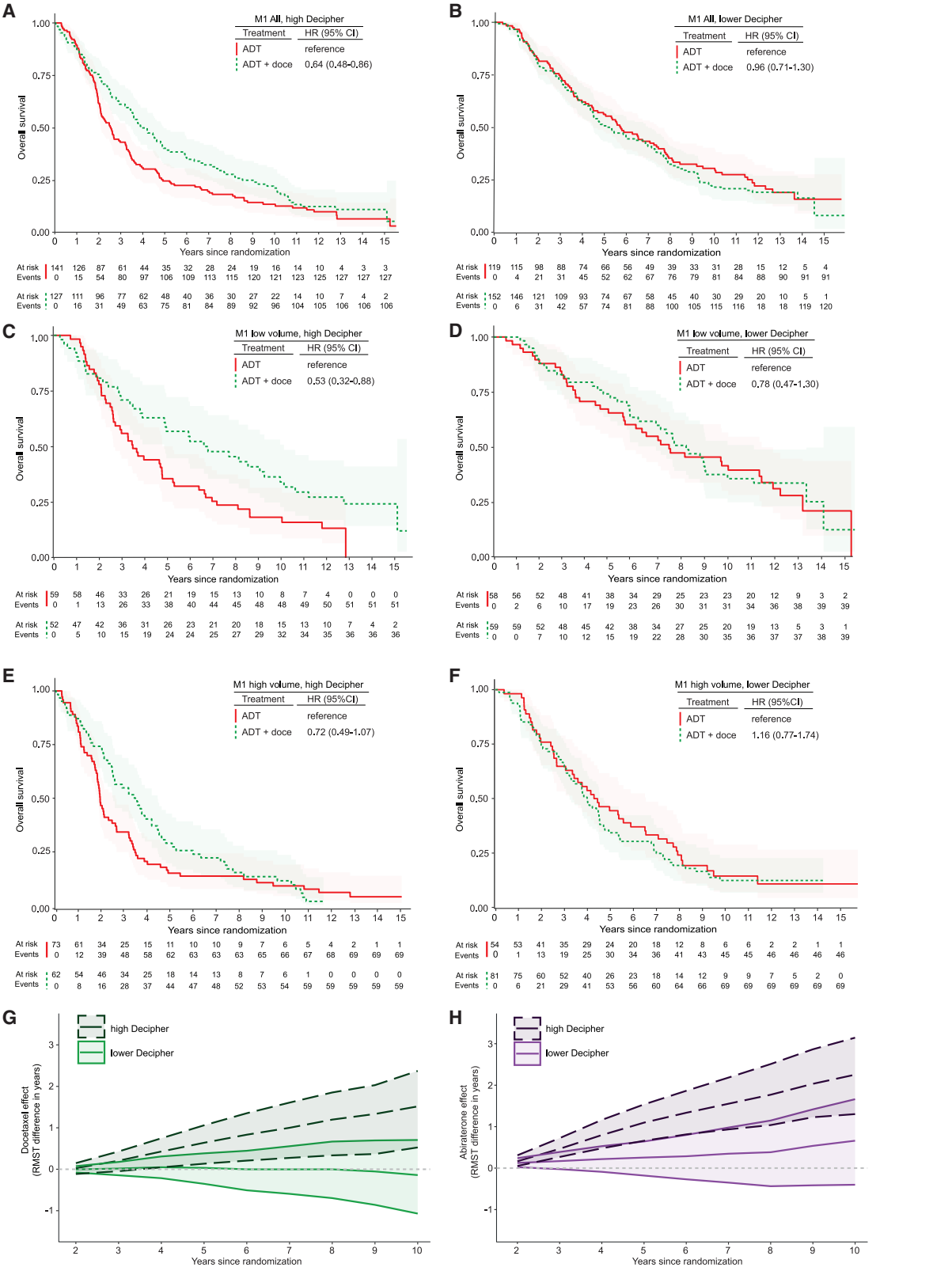

(legend on next page)

an association with survival, the association of the Basal_Zhang signature with worse outcomes was consistent with our pre-stated hypothesis (Table S7). We conclude that increased tumor AR signaling associates with longer survival in advanced prostate cancer, whereas increased proliferation captured by transcriptome signatures or the immunohistochemistry marker Ki-67 associates with shorter survival across advanced prostate cancer. Furthermore, given the STAMPEDE platform study randomized both metastatic and high-risk localized patients to the same trials, we have identified the prognostic associations of some transcriptome signatures representing different biological processes are metastatic state specific.

Primary analysis: Decipher classifier predicts benefit from docetaxel

To minimize penalization for evaluation of multiple predictive tests and therefore allow greater certainty that gene expression signatures could predict sensitivity to docetaxel or abiraterone, we pre-specified a restricted number of "primary" signatures for predictive testing prior to linking of expression and clinical data. As detailed in the "statistical analysis plan," evidence from the CHAARTED trial[20] and other studies[47] supported predictive testing of Decipher and basal-luminal subtyping (PAM50 and/or PSC for differential sensitivity with docetaxel or abiraterone) and, additionally, with AR-A_Spratt for abiraterone.

Firstly, for luminal-basal subtyping in metastatic disease, although the docetaxel effect was numerically greater in luminal B (HR 0.62, 95% CI 0.43–0.89) versus basal (HR 0.84, 95% CI 0.64–1.10), consistent with our prior analysis of the CHAARTED trial,[20] the difference did not show a statistically significant interaction effect (Table S8). There was no differential docetaxel effect in PSC subgroups, but in an analysis that pre-specified combining metastatic and non-metastatic tumors, we observed a statistically significant interaction of abiraterone with PSC luminal proliferating (HR 0.43, 95% CI 0.30–0.63) compared with PSC basal immune (HR 0.73, 95% CI 0.57–0.93, interaction $p = 0.021$) tumors. Nonetheless, both PSC groups had clinically relevant benefit from abiraterone (Table S8). The AR-A_Spratt signature did not identify a differential survival benefit with abiraterone (Table S8).

For predictive testing of the Decipher signature, we hypothesized that high Decipher scores predicted treatment benefit. We dichotomized scores ("high," >0.80; "lower," ≤0.80), pre-specified to classify metastatic patients into two equally sized groups. The lower-bound score of high Decipher tumors in the STAMPEDE cohort represents a higher threshold than used to categorize localized cancers as high risk in commercial clinical testing but is similar to the value used in the ongoing phase 3 NRG oncology GU009 trial of apalutamide intensification (ClinicalTrials.gov: NCT04513717). For patients with metastatic disease randomized in the abiraterone trial, we identified greater benefit in high Decipher (HR 0.44, 95% CI 0.32–0.62) than lower Decipher (HR 0.70, 95% CI 0.49–1.00) tumors, but this was neither statistically significant ($p = 0.061$) nor clinically relevant, given both subgroups had meaningful benefit (Tables S7 and S8; Figure S2). We did not observe a survival difference with abiraterone for high versus lower Decipher tumors from non-metastatic patients (Table S7).

By contrast, in the docetaxel trials we confirmed our primary hypothesis and identified that in patients with metastatic disease, docetaxel clinically and statistically significantly improved survival in high Decipher (HR 0.64, 95% CI 0.48–0.86) but not in lower Decipher (HR 0.96, 95% CI 0.71–1.30) tumors (biomarker-treatment interaction $p = 0.039$, Figures 5A and 5B; Tables S7 and S8). We observed associations consistent with this primary analysis in sensitivity and subgroup analyses (Table S7). For metastatic progression-free survival, we observed consistency for greater effect in metastatic patients with high Decipher tumors, but the interaction was not statistically significant (biomarker-treatment interaction $p = 0.098$, Tables S7 and S8). In non-metastatic patients, although the effect of docetaxel was numerically greater in high Decipher tumors (high, HR 0.75, 95% CI 0.44–1.28; lower, HR 1.04, 95% CI 0.68–1.59), this was neither large enough for an interaction effect (biomarker-treatment interaction $p = 0.302$) nor to clinically justify docetaxel for this population (Figure S2C; Tables S7 and S8).

Given metastatic high-volume disease has been suggested as a criterion for selecting patients for docetaxel,[48] we then demonstrated in an exploratory analysis that the direction of treatment effect prediction by the Decipher classifier was consistent (notwithstanding limited statistical precision in subgroups) in low-volume (high Decipher HR 0.53, 95% CI 0.32–0.88; lower, HR 0.78, 95% CI 0.47–1.30) and high-volume (high Decipher HR 0.72, 95% CI 0.49–1.07; lower, HR 1.16, 95% CI 0.77–1.74) metastatic disease (Figures 5C–5F; Table S7). We estimated that in patients with metastatic disease, docetaxel increased 5-year restricted mean survival times by 8 months (95% CI 2–13 months) for high Decipher tumors, compared with 0 months (95% CI −4 to 5 months) in lower Decipher tumors (Figure 5G; Table S9). This compares to the abiraterone trial in which we observed an increase in 5-year restricted mean survival time with abiraterone for metastatic patients of 13 months (95% CI 8–18 months) for high Decipher tumors and 3 months (95% CI −2 to 8 months) for lower Decipher tumors (Figure 5H; Table S9). Given the Decipher signature showed a correlation with proliferation signatures, we also tested for and found no evidence of a treatment interaction in metastatic patients for neither the CCP signature (interaction $p = 0.935$) nor Ki-67 immunohistochemistry (interaction $p = 0.340$). This suggests that increased proliferation alone does not predict docetaxel sensitivity. Overall, the Decipher classifier identified tumors with

Figure 5. Decipher classifier predicts benefit from docetaxel

Kaplan-Meier plots for patients with metastatic disease in the STAMPEDE docetaxel trials, split by pre-specified high (A) and lower (B) Decipher classifiers, and then for patients with low-volume (C and D) or high-volume (E and F) metastases ($n = 41$ excluded as metastatic volume unknown); see also Tables S7 and S8. Restricted mean survival time analyses demonstrating survival differences over time (dashed gray line marks 0 difference) by treatment allocation for patients with metastatic disease split by the Decipher classifier in the docetaxel trials (G) and in the abiraterone trial (H) relating to Table S9. Shaded areas represent 95% CI. See also Figure S2.

shorter survival when treated with ADT and abiraterone, and this class of tumors had a significant prolongation in survival when docetaxel was added to ADT.

Transcriptome classifier identifying PTEN inactivity predicts survival benefit from docetaxel

We then hypothesized that a difference in the association with survival for signatures split by treatment allocation groups could represent a differential treatment effect, which indeed was the case for the Decipher signature. After comparing the HR estimates split by patient allocation to one of the three treatment regimens evaluated in the trials, we identified that a high PTEN_loss_Liu score, representative of PTEN inactivation,[25] was strongly associated with shorter survival in patients with metastatic disease allocated to ADT or ADT with abiraterone (sdHR 1.45, 95% CI 1.19–1.77) but not in patients allocated to ADT with docetaxel (sdHR 1.01, 95% CI 0.87–1.16, Figures 6A and 6B; Table S7). This was intriguing, as it suggested that docetaxel was more effective in cancers with PTEN inactivation, which consequently did not have a shorter survival when allocated to this treatment.

PTEN inactivation can occur due to a genomic lesion or other pre-translational changes.[49] PTEN_loss_Liu was developed in prostate cancer as a continuous signature with higher scores trained to predict *PTEN* genomic loss.[25] We confirmed a bimodal distribution with a higher peak of high PTEN_loss_Liu scores in STAMPEDE tumors compared with lower-risk localized disease (Figure 6C). This is consistent with a higher prevalence of PTEN loss in more advanced disease.[12] We then compared PTEN_loss_Liu signature scores with PTEN immunohistochemistry[49] performed on an adjacent slide. We confirmed that in patients with metastatic or non-metastatic disease, an increase in PTEN_loss_Liu score[25] associated with loss of PTEN protein (Wilcoxon test: adjusted $p = 4 \times 10^{-37}$ for homogeneous loss, adjusted $p = 1 \times 10^{-27}$ for heterogeneous loss, Figure 6D). We posited that despite high overlap for cancers with both PTEN protein loss and a high PTEN_loss_Liu score, the transcriptome signature identified a distinct class of cancers with PTEN inactivity based on the downstream transcriptional effects of PTEN loss, not solely loss of expression of the gene. Using the bimodal distribution of PTEN_loss_Liu scores, we set a threshold and classified tumors with a high score as PTEN inactive, including 149/185 (81%) of patients with homogeneous PTEN protein loss, approximately equally split between non-metastatic ($n = 78$) and metastatic ($n = 71$) disease, 215/333 (65%) of patients with heterogeneous PTEN protein loss, and 187/581 (32%) positive for PTEN protein (Figure 6E). Conversely, low PTEN_loss_Liu scores were classified as PTEN active.

We then tested for prediction of a survival benefit from docetaxel in PTEN-inactive versus active tumors. This analysis was not prespecified in our statistical analysis plan and should therefore be considered exploratory. We identified a significant biomarker-docetaxel interaction (interaction $p = 0.002$) in patients with metastatic disease: PTEN inactive (HR 0.57, 95% CI 0.42–0.76) versus PTEN active (HR 1.05, 95% CI 0.77–1.43, Figures 7A and 7B; Tables S7 and S8). The same interaction effect was observed for metastatic progression-free survival (interaction $p = 0.001$, Tables S7 and S8). By contrast, there was no evidence of a biomarker interaction in non-metastatic disease (PTEN inactive, HR 1.00, 95% CI 0.62–1.61 versus PTEN active, HR 0.87, 95% CI 0.55–1.39, interaction $p = 0.669$, Figures S3A and S3B; Tables S7 and S8). Exploring this finding further, the 5-year restricted mean survival time was increased by 9 months with docetaxel (95% CI 4–13 months) in PTEN inactive metastatic disease, and there was no evidence of increased survival for any other subgroup (Figures 7C and 7D). We performed a new analysis of transcription-wide expression profiling of the CHAARTED trial biomarker cohort, and although there was insufficient power to test for a biomarker-treatment interaction, consistent with the results in the STAMPEDE trial cohort, we observed a clear and significant survival benefit from docetaxel in PTEN-inactive tumors (HR 0.52, 95% CI 0.31–0.87) but not PTEN-active cancers (HR 0.62, 95% CI 0.30–1.30) (Figures S3C and S3D). In patients with metastatic disease randomized to the STAMPEDE abiraterone trial, in contrast to the Decipher classifier, the treatment effect by the PTEN classifier was uniform (PTEN inactive, HR 0.52, 95% CI 0.36–0.73; PTEN active, HR 0.55, 95% CI 0.39–0.77; $p = 0.784$, Figures S3E and S3F; Tables S7 and S8).

Given the differences in the classification of PTEN inactivity by the PTEN_loss_Liu transcriptome classifier versus PTEN immunohistochemistry, we hypothesized that the associations with clinical outcome may be different. To address this, we repeated the docetaxel predictive multivariable analysis on the metastatic tumors with PTEN immunohistochemistry ($n = 470$). While the transcriptome classifier of PTEN inactivity retained a statistically significant biomarker-treatment interaction in this subgroup (interaction $p = 0.038$), there was no evidence of greater docetaxel benefit in tumors with heterogeneous or homogeneous loss of PTEN protein by immunohistochemistry (HR 0.85, 95% CI 0.58–1.24 for tumors with PTEN loss; interaction $p = 0.645$, Table S10). On prognostic testing, PTEN homogeneous protein loss (occurring in 13% of cancers) did not exhibit a statistically significant association with survival in metastatic disease (HR 1.24, 95% CI 0.94–1.63) but did have a significant association with survival in non-metastatic disease (HR 1.61, 95% CI 1.13–2.28, Table S10). Associations with survival for heterogeneous PTEN protein loss were consistent with homogeneous PTEN protein loss but weaker (Table S10). These analyses require validation in other datasets but suggest that while detection of homogeneous PTEN protein loss by immunohistochemistry is prognostic for non-metastatic tumors, classification of PTEN inactivity based on transcriptome expression signatures is prognostic in metastatic tumors, for which it also predicts docetaxel treatment effect.

PTEN inactivity and a high Decipher score may identify tumors with the greatest docetaxel sensitivity

Finally, given that both the Decipher and PTEN transcriptome classifiers predicted a survival benefit from docetaxel, we explored overlap. Pathway enrichment analyses of genes that correlated with PTEN_loss_Liu score identified variations in metabolism pathways (most significantly pyruvate metabolism; valine, leucine, and isoleucine degradation; and glycolysis or gluconeogenesis, all $q < 10^{-10}$). This is consistent with the previously described lipid and protein phosphatase function of PTEN[50] as a metabolic regulator, and notably, there was no overlap with pathways showing enrichment by the Decipher

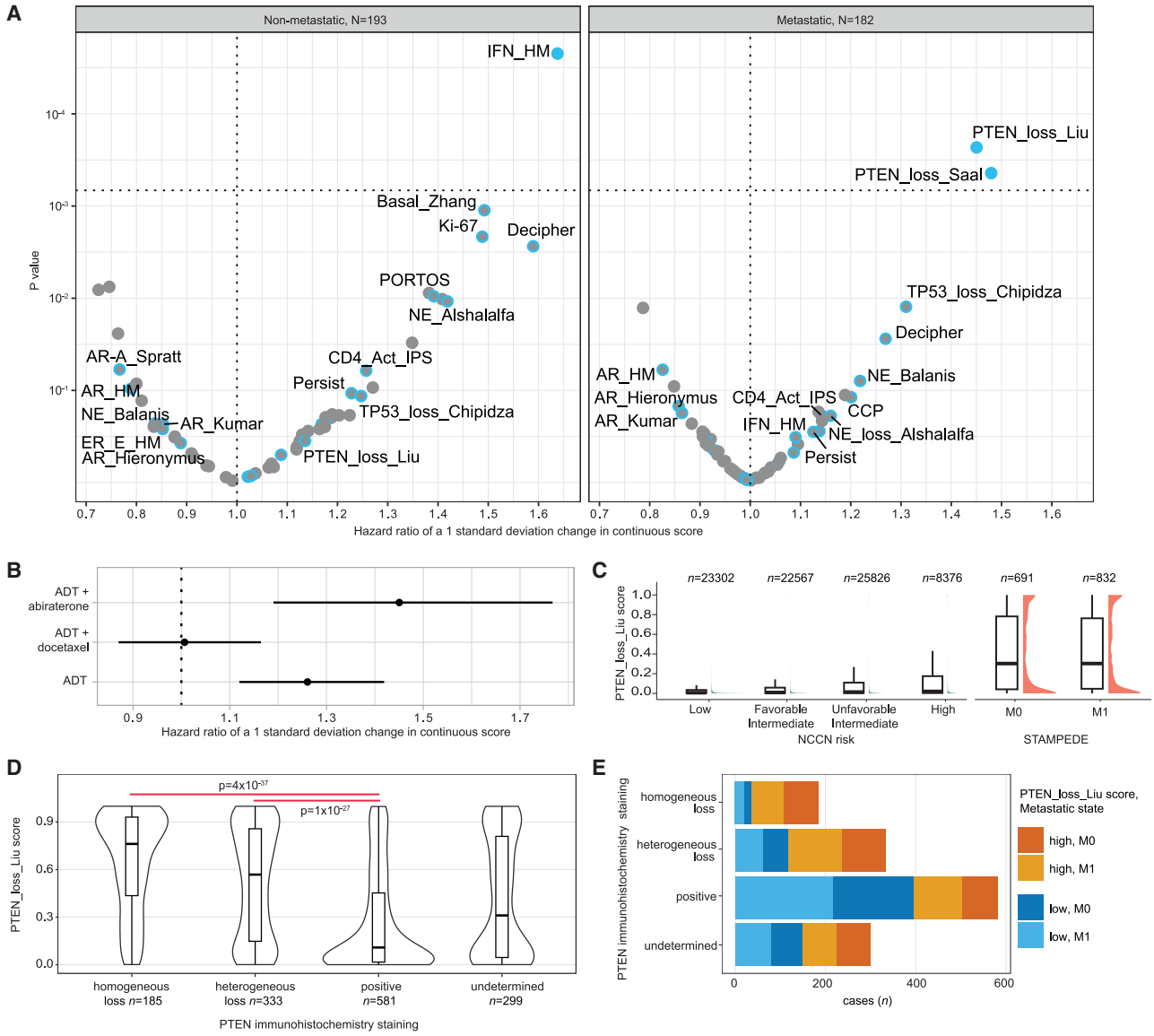

Figure 6. PTEN inactivity transcriptome signature identifies poor prognosis on abiraterone

(A) Scatterplot of HRs and *p* values from survival testing of patients allocated to ADT with abiraterone, adjusted for clinical and pathological variables, split by metastatic volume, relating to Table S7. Dots that meet statistical significance ($p < 0.00083$, marked by dashed lines) are colored blue, and other signatures or Ki-67 are gray with outline circles if statistically significant in the other metastatic state or another trial arm.

(B) Forest plots of PTEN_loss_Liu score for metastatic disease ($n = 832$), relating to Table S7.

(C) Box-and-whisker and density plots of PTEN_loss_Liu scores in localized tumors split by National Comprehensive Cancer Network (NCCN) risk categories (green) and STAMPEDE prostate tumors (salmon pink) split by M0 or M1 disease.

(D) Box-violin plots of PTEN_loss_Liu scores split by PTEN immunohistochemistry staining (*x* axis), annotated with *p* values from Wilcoxon tests.

(E) Horizontal stacked bar charts showing the number of participants in the PTEN immunohistochemistry subcohort split by PTEN_loss_Liu categorization (high, low) compared with PTEN immunohistochemistry staining split by metastatic state.

See also Figure S3.

signature (Figure 7E). Consistent with this analysis, tumors were not more likely to have high scores of both signatures, with 28% of tumors from metastatic patients assigned as both high Decipher and PTEN inactive (Figure 7F). We had insufficient power to test for a three-way predictive interaction and therefore are unable to determine whether the combined predictive effects of the two classifiers are independent, attenuated, or enhanced. However, when splitting metastatic tumors into four subgroups based on the two classifiers, we estimate that adding docetaxel for tumors classified as both high Decipher and PTEN inactive reduced the hazard of death by 45% (HR 0.55, 99% CI 0.34–0.89, Figures 7G and S3G–S3J; Table S11).

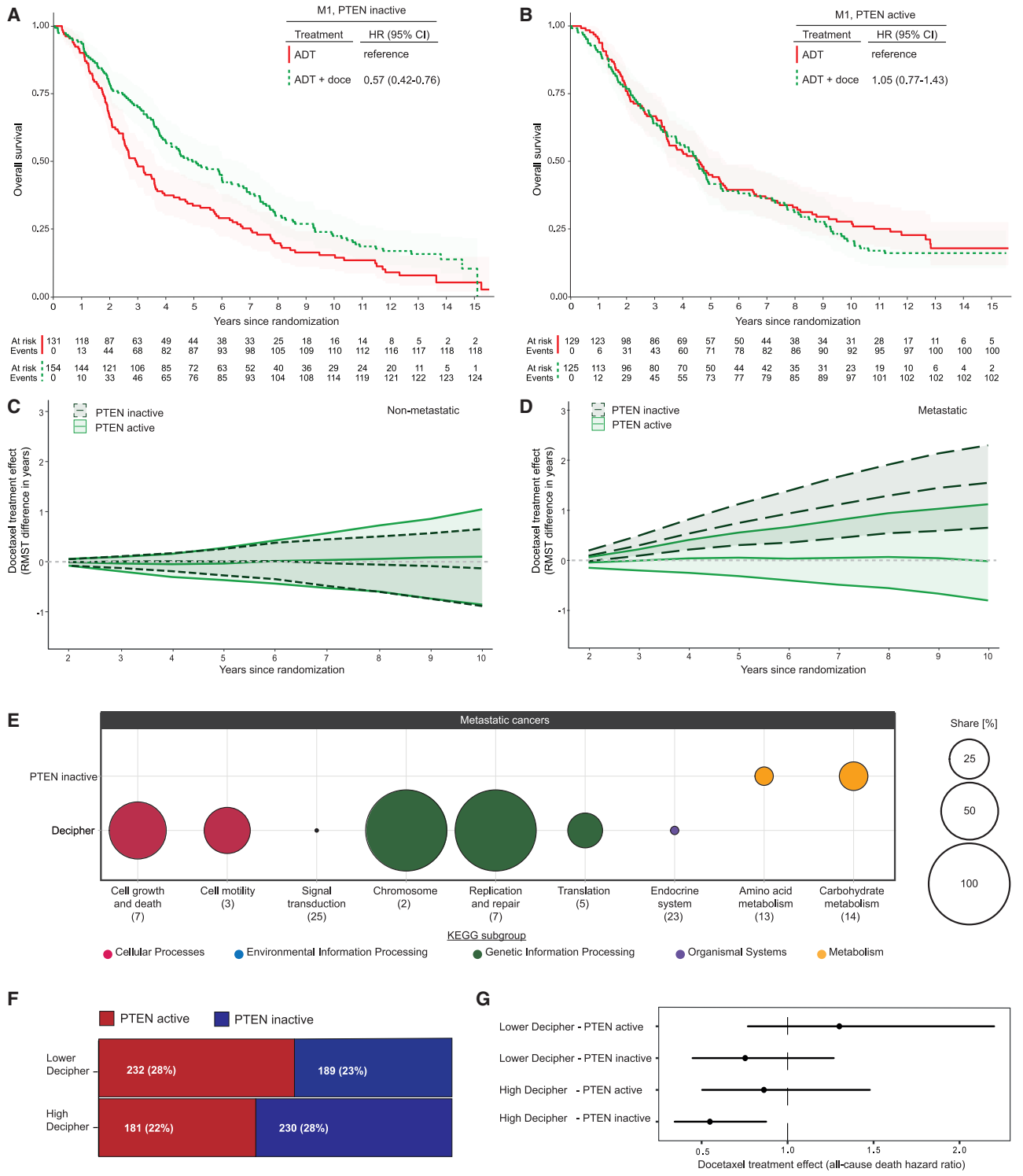

Figure 7. PTEN inactivity classifier predicts survival benefit from docetaxel in metastatic disease

(A and B) Kaplan-Meier plots of overall survival in patients with metastatic disease in the docetaxel trials, split by (A) PTEN-inactive or (B) PTEN-active tumors, relating to Tables S7 and S8. See also Table S10.

(C and D) Restricted mean survival time analyses demonstrating survival differences (dashed gray line marks 0 difference) split by PTEN inactive or active for (C) non-metastatic disease and (D) metastatic disease.

(legend continued on next page)

DISCUSSION

The premise of our study was that by linking clinical-grade transcriptome profiling with prospectively acquired survival data from directly randomized patients recruited to the STAMPEDE platform trial, we would discover predictive biomarkers and identify biological states that are associated with a distinct disease course. We confirmed that transcriptome signatures can provide clinically important information in advanced prostate cancer independent of prognostic clinical variables (including Gleason score and metastatic burden). However, we also conclude that in STAMPEDE tumors, which represent very aggressive prostate cancer and in which relatively high proliferation is observed, Ki-67 immunohistochemistry and proliferative transcriptome signatures show similarly strong associations with survival. Separately, in predictive studies, we identified clinically relevant heterogeneity of docetaxel effect in prostate cancer subtypes defined by the Decipher classifier, which represents a rational predictive biomarker for selecting patients for chemo-hormonal therapy. As we pre-specified the predicted interaction prior to linking molecular and clinical data, this test could be considered for clinical implementation.

Presently, docetaxel is sometimes combined with ADT and an ARPI (for example, abiraterone) based on physician or patient preference. Use of clinical features to guide use of docetaxel can lead to over-treatment of many patients and under-treatment of others. This is a major medical challenge given the potential detriment of docetaxel on quality of life compared with ARPI.[51] Given that both ADT and ARPI target AR activity, we posit that our discovery that the Decipher classifier identifies docetaxel-sensitive tumors treated with ADT alone (as in our study) can be extrapolated to cancers treated with ADT and an ARPI. In further support of using the Decipher test to select cancers for docetaxel, we observed shorter survival for high Decipher tumors treated with ADT and abiraterone, which therefore represent an unmet medical need that could be addressed by further treatment intensification. Decipher is a prognostic supervised-learner classifier, and we have not fully defined the mechanistic explanations for the biomarker-treatment interaction, partly given docetaxel's relatively non-targeted action. We achieved statistical rigor by limiting the number of predictive tests and using locked signatures. We also discovered that PTEN-inactive tumors are sensitive to docetaxel. PTEN has been shown to stabilize the cytoskeleton, which is therapeutically targeted by disruption of tubulin by docetaxel.[52] Given we had not pre-specified testing of PTEN inactivity as a predictive biomarker of docetaxel benefit, this result requires further evaluation. It nonetheless introduces the possibility, given the absence of overlap with the Decipher classifier, that a composite test could further improve prediction.

Transcriptome signatures, originally studied in localized breast cancer,[21,53,54] have shown potential utility for localized and biochemically recurrent prostate cancer[23,29,45,55,56] but have not been implemented in advanced prostate cancer. We conclude that this is probably a missed opportunity. Expression profiling can provide information on multiple biological processes from a single test. Next-generation sequencing has been extensively used on fresh samples, but clinically routine, formalin-fixed prostate biopsies are currently associated with a relatively high test failure rate.[57] We find consistency with prior work using single-gene assays, including the confirmation of no prognostic associations for signatures of androgen receptor splicing variant 7 (AR-v7),[31,58] CHD1-loss,[25] or ERG-positive[59] tumors. Separately, the worse outcomes on ADT or ADT and abiraterone and the differential docetaxel efficacy in metastatic disease that we observe with expression-based testing, but not immunohistochemistry for PTEN loss, may suggest additional clinical utility for using transcriptome classifiers to identify metastatic tumors for therapeutic targeting with AKT inhibition.[60]

We report robust evidence that increased AR signaling at diagnosis associates with longer survival. Conversely, canonical or non-canonical reactivation of AR signaling at progression on ADT and ARPI can drive treatment resistance and disease progression in the castration-resistant setting.[61,62] In separate work, we have used plasma DNA to identify the emergence of genomic alterations in the *AR* in at least 48% of STAMPEDE participants showing resistance after treatment with hormone intensification at the start of ADT.[63] These data illustrate how the interpretation of AR signaling as a biomarker is clinical-context specific, putatively representing disease differentiation at diagnosis and therefore longer survival, while at relapse, identifying disease reactivation secondary to resistant pathways. The lower heterogeneity in the abiraterone effect at the start of ADT could be due to the rarity of alternate AR pathway activation prior to ADT exposure. We also noted differences in associations with survival of several signatures in metastatic versus non-metastatic cancers, suggesting context specificity for the clinical implications of biological dysregulation in cancers. This included basal subtyping, previously shown to associate with poor prognosis in localized prostate cancer,[23] which does not associate with survival in metastatic disease. Notably, this conclusion is also supported by our reported significant biomarker-docetaxel interactions in metastatic but not non-metastatic disease. We have not formally tested for an interaction between differential associations with outcome by metastatic status (given this was not a pre-stated hypothesis), but these observations may explain the differential benefit from radiation or docetaxel that is observed clinically.[18,64]

(E) Circle plot demonstrating KEGG pathways that are significantly enriched with PTEN and Decipher signatures, relating to Table S6. Size of circle denotes percentage share of pathways in molecularly defined subgroup (total number of pathways in each subgroup in brackets below name). Signature genes included have a family-wise error rate (FWER) $< 1 \times 10^{-5}$.

(F) Horizontal stacked bar chart demonstrating the number (percentage proportion in brackets) of metastatic patients with prostate tumors categorized as PTEN inactive versus PTEN active and high versus lower Decipher.

(G) Forest plots of tumors split by four Decipher and PTEN inactivity classifier subgroups for patients with metastatic disease, randomized in the docetaxel trials (n = 539, whiskers for 99% simultaneous CI adjusted due to multiple subgroup testing), related to Table S11.

See also Figure S3.

As we used a clinical-grade test, our signatures are reproducible, optimized for clinical implementation, and reliably comparable across other datasets.[20,40,45] We will now make our data available as a resource for the community for further testing of biological hypotheses. Our study proposes a rational biomarker approach for selecting patients for treatment intensification with docetaxel that concurrently identifies docetaxel-sensitive cancers with shorter survival on ADT and abiraterone. In conclusion, in this large ancillary study of the STAMPEDE abiraterone and docetaxel phase 3 trials, we show that transcriptome-wide expression classifiers from primary tumors routinely acquired at diagnosis can classify advanced prostate cancers into clinically actionable groups and allow interrogation of molecular pathways that define the *in vivo* interactions of tumor biology and treatment benefit.

Roadmap to clinical implementation

We have adhered to guidelines for generating level 1B evidence in ''prospective-retrospective'' designs for biomarker discovery and evaluation.[65] (1) We included sufficient directly randomized patients for adequate statistical power. (2) The statistical analysis plan for evaluation of transcriptome classifiers was prespecified in writing before linking of molecular and clinical data. Decipher is more strongly justified for the selection of patients for docetaxel, as the direction of interaction was prestated. However, PTEN inactivity appears to show as strong an association, and future work could determine whether using both signatures improves prediction. (3) Data from a smaller but independent biomarker cohort from the CHAARTED trial were consistent. (4) The RNA values we used for generating transcriptome signature scores were from an analytically validated test on routinely acquired clinical material. Tests using the same technology are currently in routine use in localized prostate cancer and breast cancer, so the assay can be efficiently and rapidly transitioned into clinical practice. Globally, there are no other metastatic patients prospectively directly randomized to docetaxel, so supportive data could be generated in other trials that included docetaxel as standard of care (for example, ENZAMET[66] [enzalutamide in first line androgen deprivation for metastatic prostate cancer], ClinicalTrials.gov: NCT02446405) and real-world datasets, with possible prioritization of minority ethnic groups that may be under-represented in the STAMPEDE trial. Prospective assessment could also be considered and may be mandated by healthcare payers, but these studies will take many years to mature, and it may no longer be possible to randomize clinically or molecularly high-risk patient groups in a trial where docetaxel is withheld. Other signatures, such as of PTEN inactivity, are now ready for implementation in precision oncology clinical trials of targeted therapeutics.

Limitations of the study

Firstly, patient consent to allowing the collection and analysis of tissue was optional and initiated after completion of accrual. Nonetheless, the majority of participating centers contributed samples, and we included a large and consistent number of patients in all subgroups, which minimizes the risks of undetected biases related to tumor availability. Secondly, clinical practice may require immediate initiation of hormone therapies, especially in patients with high-volume metastatic disease who are more likely to be symptomatic. To ensure our cohort was representative of the full trial cohort and routine clinical practice, we included all 1,523 patients in our primary analysis but limited our conclusions to findings that were consistent in sensitivity analyses excluding patients who had received any hormone treatment prior to tumor sampling. Our findings are therefore relevant to clinical implementation and account for the effect of prior treatment. Thirdly, none of our patients (and currently no patients in any trial) were randomized to docetaxel with ADT plus ARPI as their standard of care. It is plausible that the molecular prediction of benefit for the addition of docetaxel to ADT can be extrapolated to docetaxel added to ADT and an ARPI, but this may require further validation. Fourthly, measuring gene expression using microarray technology has a reduced dynamic range compared with RNA sequencing; however, it is currently associated with a higher success rate and reproducibility on RNA from formalin-fixed, paraffin-embedded tissue to allow its use as a clinical test. Measurement of single-gene expression works when differences in expression are very large, such as ERG in ERG-positive versus -negative tumors. To test other biological signals, where variations in the expression of single genes are less, we used multi-gene signatures to maximize the signal. Fifthly, to reduce risks of false discovery, we limited these first analyses to 59 signatures, and we pre-specified our analyses before any testing of associations with outcome was undertaken (solely by trials unit statisticians). Some biological processes were represented by many signatures, while other molecular pathways may be under-represented. We mandated rigorous thresholds for statistical significance that ensure confidence in our positive results, but we cannot exclude the possibility of other clinically significant associations that we have not reported.

RESOURCE AVAILABILITY

Lead contact

Requests for resources and reagents should be directed to and will be fulfilled by the lead contact, Gerhardt Attard (g.attard@ucl.ac.uk).

Materials availability

This study did not generate new, unique reagents.

Data and code availability

Gene expression data are deposited on NCBI Gene Expression Omnibus (GEO Series accession number GSE: GSE224644). The remaining data are available within the article, supplemental information, or available from the authors upon request. Linked clinical metadata are available upon request and after pseudonymization following approval by The Medical Research Council Clinical Trials Unit (MRC CTU) at University College London (UCL) data access committee.

ACKNOWLEDGMENTS

We thank the men who were diagnosed with prostate cancer and donated their tissue to this research project. We thank the Cancer Research UK Pathology Core Facility; Alex Landless and Carla Bautista at UCL Cancer Institute; and Jason Hughes, Lisa Webber, Bashar Dabbas, and the rest of the Veracyte team for their assistance in sample processing. We thank Bart Vanhaesebroeck and Mark Linch (UCL Cancer Institute) for discussions on this manuscript. Sadly, Prof. Felix Feng died on 10th December 2024 and is greatly

missed. We acknowledge his significant contribution to prostate cancer research.

The STAMPEDE trial was funded by Cancer Research UK's Clinical Research Committee (formerly the Clinical Trials Advisory Awards Committee) with educational grants from Novartis, Sanofi-Aventis, Pfizer, Janssen Pharma NV, Astellas, and Clovis Oncology. Sanofi-Aventis, Janssen, and Novartis provided free drugs for the conduct of the trials included in this study. The MRC Clinical Trials Unit at UCL receives core funding from the Medical Research Council (grant codes MC_UU_12023/25 and MC_UU_00004/01).

The analyses in this report were primarily funded by a precision award from Prostate Cancer UK (MA-PM16-001, G.A.) with additional support from Prostate Cancer UK (MA-ETNA19-009), the Prostate Cancer Foundation (Challenge Award: 2019CHAL2729, G.A. and JBCF Young Investigator Award, E.G.), the John Black Charitable Foundation, Cancer Research UK (A22744, G.A.), Prostate Cancer Research (PRJ19GA6957), a Cancer Research UK-UCL Centre Award/Clinical Training Award (A27436, E.G.), the National Institutes of Health (R01CA238020, C.J.S. and G.A.), the Department of Defense W81XWH-19-PCRP-EIRA PC190530 PAIR (A.A.H.), the Orchid Foundation (BTXG1A1S, D.M.B.), the Benioff Initiative (F.Y.F.), and the UK National Institute for Health Research funding to the UCL Hospital's Biomedical Research Centre and Cancer Research UK funding to the City of London Centre. Transcriptome profiling was contributed by Veracyte, Inc. (San Francisco, CA, USA).

AUTHOR CONTRIBUTIONS

Conception and design: G.A. with input from E.G., H.L., D. Waugh, T.P., M.R.S., M.K.B.P., F.Y.F., C.J.S., N.W.C., and N.D.J. Obtained funding: E.G., M.R.S., M.K.B.P., A.A.H., F.Y.F., C.J.S., N.W.C., N.D.J., and G.A. Statistical analysis plan: E.G., P.D.-M., M.A.P., J.A.P., and C.B., with input from E.D., L.C.B., and G.A. STRATOSPHERE protocol: E.G., M.A.P., L. Mendes, and G.A. STAMPEDE trial management group: C.L.A., N.B.A., H.L.R., R.J.J., W.R.C., S.G., C.C.P., M.R.S., M.K.B.P., N.W.C., N.D.J., L.C.B., and G.A. Data generation: E.G., M.A.P., L. Mendes, A.S., J.A.P., A.A.H., M.I., S.H., S.F., L.D.O., Y.L., O.D., A.W., K.N., L.Z., A.U., D. Wetterskog, T.L.L., M.F., E.M.S., D.E.S., F.Y.F., and E.D. Pathology: L. Mendes, L.D.O., O.D., S.L., D.M.B., T.M., and T.L.L. Contributed patients: R.J.J., W.R.C., S.G., C.C.P., N.W.C., N.D.J., and G.A. Statistical analysis: P.D.-M., J.A.P., C.B., L. Murphy, and V.W., overseen by L.C.B. First draft of manuscript: E.G., P.D.-M., M.A.P., and G.A. Approved manuscript: all. The final interpretation of the results and decision to submit was made by the STAMPEDE trial management group. Janssen Pharma NV and Sanofi were invited to review the manuscript but played no role in data analyses.

DECLARATION OF INTERESTS

Veracyte owns intellectual property and know-how on a number of the transcriptome signatures described herein, so it could gain commercially from clinical implementation of this study's results, and UCL could receive a share of commercial revenue for its contribution to this study. E.G., L. Mendes, P.D.-M., S.H., L. Murphy, S.L., S.F., M.I., A.W., D. Wetterskog, C.L.A., H.L. R., T.M., M.F., M.K.B.P., L.C.B., and G.A. are employees of UCL. J.A.P., Y.L., and E.D. are employees of Veracyte. Y.L., J.A.P., E.D., E.G., P.D.-M., and G.A. have patent applications and/or registrations related to this work.

STAR★METHODS

Detailed methods are provided in the online version of this paper and include the following:

- KEY RESOURCES TABLE
- EXPERIMENTAL MODEL AND STUDY PARTICIPANT DETAILS
  - STAMPEDE trial cohort
  - CHAARTED trial cohort
- METHOD DETAILS
  - Study design
  - Sample retrieval and processing
  - Ki-67 staining and assessment
  - PTEN staining and assessment
  - Transcriptome expression data generation
- QUANTIFICATION AND STATISTICAL ANALYSIS
  - Generation of transcriptome signature scores
  - Pathway enrichment analysis
  - Statistical clinical outcome analyses
- ADDITIONAL RESOURCES

SUPPLEMENTAL INFORMATION

Supplemental information can be found online at https://doi.org/10.1016/j.cell.2025.07.042.

Received: January 23, 2025
Revised: June 19, 2025
Accepted: July 28, 2025
Published: August 26, 2025

REFERENCES

1. James, N.D., Tannock, I., N'Dow, J., Feng, F., Gillessen, S., Ali, S.A., Trujillo, B., Al-Lazikani, B., Attard, G., Bray, F., et al. (2024). The Lancet Commission on prostate cancer: planning for the surge in cases. Lancet *403*, 1683–1722. https://doi.org/10.1016/S0140-6736(24)00651-2.
2. Attard, G., Murphy, L., Clarke, N.W., Cross, W., Jones, R.J., Parker, C.C., Gillessen, S., Cook, A., Brawley, C., Amos, C.L., et al. (2022). Abiraterone acetate and prednisolone with or without enzalutamide for high-risk non-metastatic prostate cancer: a meta-analysis of primary results from two randomised controlled phase 3 trials of the STAMPEDE platform protocol. Lancet *399*, 447–460. https://doi.org/10.1016/S0140-6736(21)02437-5.
3. Chi, K.N., Chowdhury, S., Bjartell, A., Chung, B.H., Pereira de Santana Gomes, A.J., Given, R., Juárez, A., Merseburger, A.S., Özgüroğlu, M., Uemura, H., et al. (2021). Apalutamide in Patients With Metastatic Castration-Sensitive Prostate Cancer: Final Survival Analysis of the Randomized, Double-Blind, Phase III TITAN Study. J. Clin. Oncol. *39*, 2294–2303. https://doi.org/10.1200/JCO.20.03488.
4. Sweeney, C.J., Martin, A.J., Stockler, M.R., Begbie, S., Cheung, L., Chi, K. N., Chowdhury, S., Frydenberg, M., Horvath, L.G., Joshua, A.M., et al. (2023). Testosterone suppression plus enzalutamide versus testosterone suppression plus standard antiandrogen therapy for metastatic hormone-sensitive prostate cancer (ENZAMET): an international, open-label, randomised, phase 3 trial. Lancet Oncol. *24*, 323–334. https://doi.org/10.1016/S1470-2045(23)00063-3.
5. Armstrong, A.J., Azad, A.A., Iguchi, T., Szmulewitz, R.Z., Petrylak, D.P., Holzbeierlein, J., Villers, A., Alcaraz, A., Alekseev, B., Shore, N.D., et al. (2022). Improved Survival With Enzalutamide in Patients With Metastatic Hormone-Sensitive Prostate Cancer. J. Clin. Oncol. *40*, 1616–1622. https://doi.org/10.1200/JCO.22.00193.
6. Attard, G., Murphy, L., Clarke, N.W., Sachdeva, A., Jones, C., Hoyle, A., Cross, W., Jones, R.J., Parker, C.C., Gillessen, S., et al. (2023). Abiraterone acetate plus prednisolone with or without enzalutamide for patients with metastatic prostate cancer starting androgen deprivation therapy: final results from two randomised phase 3 trials of the STAMPEDE platform protocol. Lancet Oncol. *24*, 443–456. https://doi.org/10.1016/S1470-2045(23)00148-1.
7. Fizazi, K., Tran, N., Fein, L., Matsubara, N., Rodriguez-Antolin, A., Alekseev, B.Y., Özgüroğlu, M., Ye, D., Feyerabend, S., Protheroe, A., et al. (2019). Abiraterone acetate plus prednisone in patients with newly diagnosed high-risk metastatic castration-sensitive prostate cancer (LATITUDE): final overall survival analysis of a randomised, double-blind, phase 3 trial. Lancet Oncol. *20*, 686–700. https://doi.org/10.1016/S1470-2045(19)30082-8.
8. Fizazi, K., Foulon, S., Carles, J., Roubaud, G., McDermott, R., Fléchon, A., Tombal, B., Supiot, S., Berthold, D., Ronchin, P., et al. (2022). Abiraterone

plus prednisone added to androgen deprivation therapy and docetaxel in de novo metastatic castration-sensitive prostate cancer (PEACE-1): a multicentre, open-label, randomised, phase 3 study with a 2 × 2 factorial design. Lancet *399*, 1695–1707. https://doi.org/10.1016/S0140-6736(22)00367-1.

9. Smith, M.R., Hussain, M., Saad, F., Fizazi, K., Sternberg, C.N., Crawford, E.D., Kopyltsov, E., Park, C.H., Alekseev, B., Montesa-Pino, Á., et al. (2022). Darolutamide and Survival in Metastatic, Hormone-Sensitive Prostate Cancer. N. Engl. J. Med. *386*, 1132–1142. https://doi.org/10.1056/NEJMoa2119115.
10. James, N.D., Sydes, M.R., Clarke, N.W., Mason, M.D., Dearnaley, D.P., Spears, M.R., Ritchie, A.W.S., Parker, C.C., Russell, J.M., Attard, G., et al. (2016). Addition of docetaxel, zoledronic acid, or both to first-line long-term hormone therapy in prostate cancer (STAMPEDE): survival results from an adaptive, multiarm, multistage, platform randomised controlled trial. Lancet *387*, 1163–1177. https://doi.org/10.1016/S0140-6736(15)01037-5.
11. Sweeney, C.J., Chen, Y.H., Carducci, M., Liu, G., Jarrard, D.F., Eisenberger, M., Wong, Y.N., Hahn, N., Kohli, M., Cooney, M.M., et al. (2015). Chemohormonal Therapy in Metastatic Hormone-Sensitive Prostate Cancer. N. Engl. J. Med. *373*, 737–746. https://doi.org/10.1056/NEJMoa1503747.
12. Hamid, A.A., Gray, K.P., Shaw, G., MacConaill, L.E., Evan, C., Bernard, B., Loda, M., Corcoran, N.M., Van Allen, E.M., Choudhury, A.D., et al. (2019). Compound Genomic Alterations of TP53, PTEN, and RB1 Tumor Suppressors in Localized and Metastatic Prostate Cancer. Eur. Urol. *76*, 89–97. https://doi.org/10.1016/j.eururo.2018.11.045.
13. Swami, U., Graf, R.P., Nussenzveig, R.H., Fisher, V., Tukachinsky, H., Schrock, A.B., Li, G., Ross, J.S., Sayegh, N., Tripathi, N., et al. (2022). SPOP Mutations as a Predictive Biomarker for Androgen Receptor Axis-Targeted Therapy in De Novo Metastatic Castration-Sensitive Prostate Cancer. Clin. Cancer Res. *28*, 4917–4925. https://doi.org/10.1158/1078-0432.CCR-22-2228.
14. Adamo, P., and Ladomery, M.R. (2016). The oncogene ERG: a key factor in prostate cancer. Oncogene *35*, 403–414. https://doi.org/10.1038/onc.2015.109.
15. Conteduca, V., Wetterskog, D., Sharabiani, M.T.A., Grande, E., Fernandez-Perez, M.P., Jayaram, A., Salvi, S., Castellano, D., Romanel, A., Lolli, C., et al. (2017). Androgen receptor gene status in plasma DNA associates with worse outcome on enzalutamide or abiraterone for castration-resistant prostate cancer: a multi-institution correlative biomarker study. Ann. Oncol. *28*, 1508–1516. https://doi.org/10.1093/annonc/mdx155.
16. Romanel, A., Gasi Tandefelt, D., Conteduca, V., Jayaram, A., Casiraghi, N., Wetterskog, D., Salvi, S., Amadori, D., Zafeiriou, Z., Rescigno, P., et al. (2015). Plasma AR and abiraterone-resistant prostate cancer. Sci. Transl. Med. *7*, 312re310. https://doi.org/10.1126/scitranslmed.aac9511.
17. Clarke, N.W., Ali, A., Ingleby, F.C., Hoyle, A., Amos, C.L., Attard, G., Brawley, C.D., Calvert, J., Chowdhury, S., Cook, A., et al. (2019). Addition of docetaxel to hormonal therapy in low- and high-burden metastatic hormone sensitive prostate cancer: long-term survival results from the STAMPEDE trial. Ann. Oncol. *30*, 1992–2003. https://doi.org/10.1093/annonc/mdz396.
18. James, N.D., Ingleby, F.C., Clarke, N.W., Amos, C.L., Attard, G., Brawley, C.D., Chowdhury, S., Cross, W., Dearnaley, D.P., Gilbert, D.C., et al. (2022). Docetaxel for Nonmetastatic Prostate Cancer: Long-Term Survival Outcomes in the STAMPEDE Randomized Controlled Trial. JNCI Cancer Spectr. *6*, pkac043. https://doi.org/10.1093/jncics/pkac043.
19. James, N.D., de Bono, J.S., Spears, M.R., Clarke, N.W., Mason, M.D., Dearnaley, D.P., Ritchie, A.W.S., Amos, C.L., Gilson, C., Jones, R.J., et al. (2017). Abiraterone for Prostate Cancer Not Previously Treated with Hormone Therapy. N. Engl. J. Med. *377*, 338–351. https://doi.org/10.1056/NEJMoa1702900.
20. Hamid, A.A., Huang, H.C., Wang, V., Chen, Y.H., Feng, F., Den, R., Attard, G., Van Allen, E.M., Tran, P.T., Spratt, D.E., et al. (2021). Transcriptional profiling of primary prostate tumor in metastatic hormone-sensitive prostate cancer and association with clinical outcomes: correlative analysis of the E3805 CHAARTED trial. Ann. Oncol. *32*, 1157–1166. https://doi.org/10.1016/j.annonc.2021.06.003.
21. Parker, J.S., Mullins, M., Cheang, M.C.U., Leung, S., Voduc, D., Vickery, T., Davies, S., Fauron, C., He, X., Hu, Z., et al. (2009). Supervised risk predictor of breast cancer based on intrinsic subtypes. J. Clin. Oncol. *27*, 1160–1167. https://doi.org/10.1200/JCO.2008.18.1370.
22. Weiner, A.B., Liu, Y., Hakansson, A., Zhao, X., Proudfoot, J.A., Ho, J., Zhang, J.H., Li, E.V., Karnes, R.J., Den, R.B., et al. (2023). A novel prostate cancer subtyping classifier based on luminal and basal phenotypes. Cancer *129*, 2169–2178. https://doi.org/10.1002/cncr.34790.
23. Zhao, S.G., Chang, S.L., Erho, N., Yu, M., Lehrer, J., Alshalalfa, M., Speers, C., Cooperberg, M.R., Kim, W., Ryan, C.J., et al. (2017). Associations of Luminal and Basal Subtyping of Prostate Cancer With Prognosis and Response to Androgen Deprivation Therapy. JAMA Oncol. *3*, 1663–1672. https://doi.org/10.1001/jamaoncol.2017.0751.
24. Setlur, S.R., Mertz, K.D., Hoshida, Y., Demichelis, F., Lupien, M., Perner, S., Sboner, A., Pawitan, Y., Andrén, O., Johnson, L.A., et al. (2008). Estrogen-dependent signaling in a molecularly distinct subclass of aggressive prostate cancer. J. Natl. Cancer Inst. *100*, 815–825. https://doi.org/10.1093/jnci/djn150.
25. Liu, D., Augello, M.A., Grbesa, I., Prandi, D., Liu, Y., Shoag, J.E., Karnes, R.J., Trock, B.J., Klein, E.A., Den, R.B., et al. (2021). Tumor subtype defines distinct pathways of molecular and clinical progression in primary prostate cancer. J. Clin. Invest. *131*, e147878. https://doi.org/10.1172/JCI147878.
26. Saal, L.H., Johansson, P., Holm, K., Gruvberger-Saal, S.K., She, Q.B., Maurer, M., Koujak, S., Ferrando, A.A., Malmström, P., Memeo, L., et al. (2007). Poor prognosis in carcinoma is associated with a gene expression signature of aberrant PTEN tumor suppressor pathway activity. Proc. Natl. Acad. Sci. USA *104*, 7564–7569. https://doi.org/10.1073/pnas.0702507104.
27. Chipidza, F.E., Alshalalfa, M., Mahal, B.A., Karnes, R.J., Liu, Y., Davicioni, E., Martin, N.E., Mouw, K.W., Feng, F.Y., Nguyen, P.L., et al. (2021). Development and Validation of a Novel TP53 Mutation Signature That Predicts Risk of Metastasis in Primary Prostate Cancer. Clin. Genitourin. Cancer *19*, 246–254.e5. https://doi.org/10.1016/j.clgc.2020.08.004.
28. Donehower, L.A., Soussi, T., Korkut, A., Liu, Y., Schultz, A., Cardenas, M., Li, X., Babur, O., Hsu, T.K., Lichtarge, O., et al. (2019). Integrated Analysis of TP53 Gene and Pathway Alterations in The Cancer Genome Atlas. Cell Rep. *28*, 1370–1384.e5. https://doi.org/10.1016/j.celrep.2019.07.001.
29. Spratt, D.E., Alshalalfa, M., Fishbane, N., Weiner, A.B., Mehra, R., Mahal, B.A., Lehrer, J., Liu, Y., Zhao, S.G., Speers, C., et al. (2019). Transcriptomic Heterogeneity of Androgen Receptor Activity Defines a de novo low AR-Active Subclass in Treatment Naive Primary Prostate Cancer. Clin. Cancer Res. *25*, 6721–6730. https://doi.org/10.1158/1078-0432.CCR-19-1587.
30. Karnes, R.J., Sharma, V., Choeurng, V., Ashab, H.A.D., Erho, N., Alshalalfa, M., Trock, B., Ross, A., Yousefi, K., Tsai, H., et al. (2018). Development and Validation of a Prostate Cancer Genomic Signature that Predicts Early ADT Treatment Response Following Radical Prostatectomy. Clin. Cancer Res. *24*, 3908–3916. https://doi.org/10.1158/1078-0432.CCR-17-2745.
31. Sharp, A., Coleman, I., Yuan, W., Sprenger, C., Dolling, D., Rodrigues, D.N., Russo, J.W., Figueiredo, I., Bertan, C., Seed, G., et al. (2019). Androgen receptor splice variant-7 expression emerges with castration resistance in prostate cancer. J. Clin. Invest. *129*, 192–208. https://doi.org/10.1172/JCI122819.
32. Hieronymus, H., Lamb, J., Ross, K.N., Peng, X.P., Clement, C., Rodina, A., Nieto, M., Du, J., Stegmaier, K., Raj, S.M., et al. (2006). Gene expression signature-based chemical genomic prediction identifies a novel class of HSP90 pathway modulators. Cancer Cell *10*, 321–330. https://doi.org/10.1016/j.ccr.2006.09.005.

33. Liberzon, A., Birger, C., Thorvaldsdóttir, H., Ghandi, M., Mesirov, J.P., and Tamayo, P. (2015). The Molecular Signatures Database (MSigDB) hallmark gene set collection. Cell Syst. *1*, 417–425. https://doi.org/10.1016/j.cels.2015.12.004.

34. Kumar, A., Coleman, I., Morrissey, C., Zhang, X., True, L.D., Gulati, R., Etzioni, R., Bolouri, H., Montgomery, B., White, T., et al. (2016). Substantial interindividual and limited intraindividual genomic diversity among tumors from men with metastatic prostate cancer. Nat. Med. *22*, 369–378. https://doi.org/10.1038/nm.4053.

35. Alshalalfa, M., Liu, Y., Wyatt, A.W., Gibb, E.A., Tsai, H.K., Erho, N., Lehrer, J., Takhar, M., Ramnarine, V.R., Collins, C.C., et al. (2019). Characterization of transcriptomic signature of primary prostate cancer analogous to prostatic small cell neuroendocrine carcinoma. Int. J. Cancer *145*, 3453–3461. https://doi.org/10.1002/ijc.32430.

36. Balanis, N.G., Sheu, K.M., Esedebe, F.N., Patel, S.J., Smith, B.A., Park, J.W., Alhani, S., Gomperts, B.N., Huang, J., Witte, O.N., et al. (2019). Pan-cancer Convergence to a Small-Cell Neuroendocrine Phenotype that Shares Susceptibilities with Hematological Malignancies. Cancer Cell *36*, 17–34.e7. https://doi.org/10.1016/j.ccell.2019.06.005.

37. Beltran, H., Prandi, D., Mosquera, J.M., Benelli, M., Puca, L., Cyrta, J., Marotz, C., Giannopoulou, E., Chakravarthi, B.V.S.K., Varambally, S., et al. (2016). Divergent clonal evolution of castration-resistant neuroendocrine prostate cancer. Nat. Med. *22*, 298–305. https://doi.org/10.1038/nm.4045.

38. Tsai, H.K., Lehrer, J., Alshalalfa, M., Erho, N., Davicioni, E., and Lotan, T.L. (2017). Gene expression signatures of neuroendocrine prostate cancer and primary small cell prostatic carcinoma. BMC Cancer *17*, 759. https://doi.org/10.1186/s12885-017-3729-z.

39. Aggarwal, R., Rydzewski, N.R., Zhang, L., Foye, A., Kim, W., Helzer, K.T., Bakhtiar, H., Chang, S.L., Perry, M.D., Gleave, M., et al. (2021). Prognosis Associated With Luminal and Basal Subtypes of Metastatic Prostate Cancer. JAMA Oncol. *7*, 1644–1652. https://doi.org/10.1001/jamaoncol.2021.3987.

40. Nguyen, P.L., Huang, H.R., Spratt, D.E., Davicioni, E., Sandler, H.M., Shipley, W.U., Efstathiou, J.A., Simko, J.P., Pollack, A., Dicker, A.P., et al. (2023). Analysis of a Biopsy-Based Genomic Classifier in High-Risk Prostate Cancer: Meta-Analysis of the NRG Oncology/Radiation Therapy Oncology Group 9202, 9413, and 9902 Phase 3 Randomized Trials. Int. J. Radiat. Oncol. Biol. Phys. *116*, 521–529. https://doi.org/10.1016/j.ijrobp.2022.12.035.

41. Cuzick, J., Swanson, G.P., Fisher, G., Brothman, A.R., Berney, D.M., Reid, J.E., Mesher, D., Speights, V.O., Stankiewicz, E., Foster, C.S., et al. (2011). Prognostic value of an RNA expression signature derived from cell cycle proliferation genes in patients with prostate cancer: a retrospective study. Lancet Oncol. *12*, 245–255. https://doi.org/10.1016/S1470-2045(10)70295-3.

42. Carter, S.L., Eklund, A.C., Kohane, I.S., Harris, L.N., and Szallasi, Z. (2006). A signature of chromosomal instability inferred from gene expression profiles predicts clinical outcome in multiple human cancers. Nat. Genet. *38*, 1043–1048. https://doi.org/10.1038/ng1861.

43. Weiner, A.B., Liu, Y., McFarlane, M., Bawa, P.S., Li, E.V., Zhao, X., Li, Z., Hammoud, T., Hazime, M., Karnes, R.J., et al. (2022). A transcriptomic model for homologous recombination deficiency in prostate cancer. Prostate Cancer Prostatic Dis. *25*, 659–665. https://doi.org/10.1038/s41391-021-00416-2.

44. Taavitsainen, S., Engedal, N., Cao, S., Handle, F., Erickson, A., Prekovic, S., Wetterskog, D., Tolonen, T., Vuorinen, E.M., Kiviaho, A., et al. (2021). Single-cell ATAC and RNA sequencing reveal pre-existing and persistent cells associated with prostate cancer relapse. Nat. Commun. *12*, 5307. https://doi.org/10.1038/s41467-021-25624-1.

45. Zhao, S.G., Chang, S.L., Spratt, D.E., Erho, N., Yu, M., Ashab, H.A.D., Alshalalfa, M., Speers, C., Tomlins, S.A., Davicioni, E., et al. (2016). Development and validation of a 24-gene predictor of response to postoperative radiotherapy in prostate cancer: a matched, retrospective analysis. Lancet Oncol. *17*, 1612–1620. https://doi.org/10.1016/S1470-2045(16)30491-0.

46. Zhang, D., Park, D., Zhong, Y., Lu, Y., Rycaj, K., Gong, S., Chen, X., Liu, X., Chao, H.P., Whitney, P., et al. (2016). Stem cell and neurogenic gene-expression profiles link prostate basal cells to aggressive prostate cancer. Nat. Commun. *7*, 10798. https://doi.org/10.1038/ncomms10798.

47. Feng, F.Y., Huang, H.C., Spratt, D.E., Zhao, S.G., Sandler, H.M., Simko, J.P., Davicioni, E., Nguyen, P.L., Pollack, A., Efstathiou, J.A., et al. (2021). Validation of a 22-Gene Genomic Classifier in Patients With Recurrent Prostate Cancer: An Ancillary Study of the NRG/RTOG 9601 Randomized Clinical Trial. JAMA Oncol. *7*, 544–552. https://doi.org/10.1001/jamaoncol.2020.7671.

48. Vale, C.L., Fisher, D.J., Godolphin, P.J., Rydzewska, L.H., Boher, J.M., Burdett, S., Chen, Y.H., Clarke, N.W., Fizazi, K., Gravis, G., et al. (2023). Which patients with metastatic hormone-sensitive prostate cancer benefit from docetaxel: a systematic review and meta-analysis of individual participant data from randomised trials. Lancet Oncol. *24*, 783–797. https://doi.org/10.1016/S1470-2045(23)00230-9.

49. Lotan, T.L., Gurel, B., Sutcliffe, S., Esopi, D., Liu, W., Xu, J., Hicks, J.L., Park, B.H., Humphreys, E., Partin, A.W., et al. (2011). PTEN protein loss by immunostaining: analytic validation and prognostic indicator for a high risk surgical cohort of prostate cancer patients. Clin. Cancer Res. *17*, 6563–6573. https://doi.org/10.1158/1078-0432.CCR-11-1244.

50. Chen, C.Y., Chen, J., He, L., and Stiles, B.L. (2018). PTEN: Tumor Suppressor and Metabolic Regulator. Front. Endocrinol. (Lausanne) *9*, 338. https://doi.org/10.3389/fendo.2018.00338.

51. Rush, H.L., Murphy, L., Morgans, A.K., Clarke, N.W., Cook, A.D., Attard, G., Macnair, A., Dearnaley, D.P., Parker, C.C., Russell, J.M., et al. (2022). Quality of Life in Men With Prostate Cancer Randomly Allocated to Receive Docetaxel or Abiraterone in the STAMPEDE Trial. J. Clin. Oncol. *40*, 825–836. https://doi.org/10.1200/JCO.21.00728.

52. Kath, C., Goni-Oliver, P., Müller, R., Schultz, C., Haucke, V., Eickholt, B., and Schmoranzer, J. (2018). PTEN suppresses axon outgrowth by down-regulating the level of detyrosinated microtubules. PLoS One *13*, e0193257. https://doi.org/10.1371/journal.pone.0193257.

53. Sørlie, T., Perou, C.M., Tibshirani, R., Aas, T., Geisler, S., Johnsen, H., Hastie, T., Eisen, M.B., van de Rijn, M., Jeffrey, S.S., et al. (2001). Gene expression patterns of breast carcinomas distinguish tumor subclasses with clinical implications. Proc. Natl. Acad. Sci. USA *98*, 10869–10874. https://doi.org/10.1073/pnas.191367098.

54. Rueda, O.M., Sammut, S.J., Seoane, J.A., Chin, S.F., Caswell-Jin, J.L., Callari, M., Batra, R., Pereira, B., Bruna, A., Ali, H.R., et al. (2019). Dynamics of breast-cancer relapse reveal late-recurring ER-positive genomic subgroups. Nature *567*, 399–404. https://doi.org/10.1038/s41586-019-1007-8.

55. Erho, N., Crisan, A., Vergara, I.A., Mitra, A.P., Ghadessi, M., Buerki, C., Bergstralh, E.J., Kollmeyer, T., Fink, S., Haddad, Z., et al. (2013). Discovery and validation of a prostate cancer genomic classifier that predicts early metastasis following radical prostatectomy. PLoS One *8*, e66855. https://doi.org/10.1371/journal.pone.0066855.

56. Dal Pra, A., Ghadjar, P., Hayoz, S., Liu, V.Y.T., Spratt, D.E., Thompson, D.J.S., Davicioni, E., Huang, H.C., Zhao, X., Liu, Y., et al. (2022). Validation of the Decipher genomic classifier in patients receiving salvage radiotherapy without hormone therapy after radical prostatectomy - an ancillary study of the SAKK 09/10 randomized clinical trial. Ann. Oncol. *33*, 950–958. https://doi.org/10.1016/j.annonc.2022.05.007.

57. Gilson, C., Ingleby, F., Gilbert, D.C., Parry, M.A., Atako, N.B., Ali, A., Hoyle, A., Clarke, N.W., Gannon, M., Wanstall, C., et al. (2020). Genomic Profiles of De Novo High- and Low-Volume Metastatic Prostate Cancer: Results From a 2-Stage Feasibility and Prevalence Study in the STAMPEDE Trial. JCO Precis. Oncol. *4*, 882–897. https://doi.org/10.1200/PO.19.00388.

58. Sowalsky, A.G., Figueiredo, I., Lis, R.T., Coleman, I., Gurel, B., Bogdan, D., Yuan, W., Russo, J.W., Bright, J.R., Whitlock, N.C., et al. (2022). Assessment of Androgen Receptor Splice Variant-7 as a Biomarker of Clinical

Response in Castration-Sensitive Prostate Cancer. Clin. Cancer Res. *28*, 3509–3525. https://doi.org/10.1158/1078-0432.CCR-22-0851.

59. Pettersson, A., Graff, R.E., Bauer, S.R., Pitt, M.J., Lis, R.T., Stack, E.C., Martin, N.E., Kunz, L., Penney, K.L., Ligon, A.H., et al. (2012). The TMPRSS2:ERG rearrangement, ERG expression, and prostate cancer outcomes: a cohort study and meta-analysis. Cancer Epidemiol. Biomarkers Prev. *21*, 1497–1509. https://doi.org/10.1158/1055-9965.EPI-12-0042.
60. Sweeney, C., Bracarda, S., Sternberg, C.N., Chi, K.N., Olmos, D., Sandhu, S., Massard, C., Matsubara, N., Alekseev, B., Parnis, F., et al. (2021). Ipatasertib plus abiraterone and prednisolone in metastatic castration-resistant prostate cancer (IPATential150): a multicentre, randomised, double-blind, phase 3 trial. Lancet *398*, 131–142. https://doi.org/10.1016/S0140-6736(21)00580-8.
61. He, Y., Wei, T., Ye, Z., Orme, J.J., Lin, D., Sheng, H., Fazli, L., Jeffrey Karnes, R., Jimenez, R., Wang, L., et al. (2021). A noncanonical AR addiction drives enzalutamide resistance in prostate cancer. Nat. Commun. *12*, 1521. https://doi.org/10.1038/s41467-021-21860-7.
62. Lawrence, M.G., Keerthikumar, S., Townley, S.L., Clark, A.K., Cuffe, G.B., Laven-Law, G., Hanson, A.R., Shrestha, R.K., Knutson, T.P., Richards, M. G., et al. (2025). Reprogramming of Androgen Receptor Activity in Castration-resistant Prostate Cancer is Shaped by Truncated Variants. Published online April 10, 2025. Eur. Urol. Focus. S2405-4569(25)00073-2. https://doi.org/10.1016/j.euf.2025.03.017.
63. Leone, G., Orlando, F., Dutey-Magni, P., Vainauskas, O., Grist, E., Ciani, Y., Lall, S., Thakali, S., Wingate, A., Wetterskog, D., et al. (2025). Plasma AR Alterations and Timing of Intensified Hormone Treatment for Prostate Cancer: the STAMPEDE Phase 3 Randomized Clinical Trial. JAMA Oncol. *11*, 426–429. https://doi.org/10.1001/jamaoncol.2024.7051.
64. Parker, C.C., James, N.D., Brawley, C.D., Clarke, N.W., Hoyle, A.P., Ali, A., Ritchie, A.W.S., Attard, G., Chowdhury, S., Cross, W., et al. (2018). Radiotherapy to the primary tumour for newly diagnosed, metastatic prostate cancer (STAMPEDE): a randomised controlled phase 3 trial. Lancet *392*, 2353–2366. https://doi.org/10.1016/S0140-6736(18)32486-3.
65. Simon, R.M., Paik, S., and Hayes, D.F. (2009). Use of Archived Specimens in Evaluation of Prognostic and Predictive Biomarkers. J. Natl. Cancer Inst. *101*, 1446–1452. https://doi.org/10.1093/jnci/djp335.
66. Davis, I.D., Martin, A.J., Stockler, M.R., Begbie, S., Chi, K.N., Chowdhury, S., Coskinas, X., Frydenberg, M., Hague, W.E., Horvath, L.G., et al. (2019). Enzalutamide with Standard First-Line Therapy in Metastatic Prostate Cancer. N. Engl. J. Med. *381*, 121–131. https://doi.org/10.1056/NEJMoa1903835.
67. Hoyle, A.P., Ali, A., James, N.D., Cook, A., Parker, C.C., de Bono, J.S., Attard, G., Chowdhury, S., Cross, W.R., Dearnaley, D.P., et al. (2019). Abiraterone in "High-" and "Low-risk" Metastatic Hormone-sensitive Prostate Cancer. Eur. Urol. *76*, 719–728. https://doi.org/10.1016/j.eururo.2019.08.006.
68. Grist, E., Friedrich, S., Brawley, C., Mendes, L., Parry, M., Ali, A., Haran, A., Hoyle, A., Gilson, C., Lall, S., et al. (2022). Accumulation of copy number alterations and clinical progression across advanced prostate cancer. Genome Med. *14*, 102. https://doi.org/10.1186/s13073-022-01080-4.
69. Berney, D.M., Gopalan, A., Kudahetti, S., Fisher, G., Ambroisine, L., Foster, C.S., Reuter, V., Eastham, J., Moller, H., Kattan, M.W., et al. (2009). Ki-67 and outcome in clinically localised prostate cancer: analysis of conservatively treated prostate cancer patients from the Trans-Atlantic Prostate Group study. Br. J. Cancer *100*, 888–893. https://doi.org/10.1038/sj.bjc.6604951.
70. Kammerer-Jacquet, S.F., Ahmad, A., Møller, H., Sandu, H., Scardino, P., Soosay, G., Beltran, L., Cuzick, J., and Berney, D.M. (2019). Ki-67 is an independent predictor of prostate cancer death in routine needle biopsy samples: proving utility for routine assessments. Mod. Pathol. *32*, 1303–1309. https://doi.org/10.1038/s41379-019-0268-y.
71. Gautier, L., Cope, L., Bolstad, B.M., and Irizarry, R.A. (2004). affy–analysis of Affymetrix GeneChip data at the probe level. Bioinformatics *20*, 307–315. https://doi.org/10.1093/bioinformatics/btg405.
72. Piccolo, S.R., Sun, Y., Campbell, J.D., Lenburg, M.E., Bild, A.H., and Johnson, W.E. (2012). A single-sample microarray normalization method to facilitate personalized-medicine workflows. Genomics *100*, 337–344. https://doi.org/10.1016/j.ygeno.2012.08.003.
73. Benjamini, Y., and Hochberg, Y. (2018). Controlling the False Discovery Rate: A Practical and Powerful Approach to Multiple Testing. J. R. Stat. Soc. Series B Stat Methodol. *57*, 289–300. https://doi.org/10.1111/j.2517-6161.1995.tb02031.x.
74. Durinck, S., Moreau, Y., Kasprzyk, A., Davis, S., De Moor, B., Brazma, A., and Huber, W. (2005). BioMart and Bioconductor: a powerful link between biological databases and microarray data analysis. Bioinformatics *21*, 3439–3440. https://doi.org/10.1093/bioinformatics/bti525.
75. Durinck, S., Spellman, P.T., Birney, E., and Huber, W. (2009). Mapping identifiers for the integration of genomic datasets with the R/Bioconductor package biomaRt. Nat. Protoc. *4*, 1184–1191. https://doi.org/10.1038/nprot.2009.97.
76. Ogris, C., Castresana-Aguirre, M., and Sonnhammer, E.L.L. (2022). PathwAX II: network-based pathway analysis with interactive visualization of network crosstalk. Bioinformatics *38*, 2659–2660. https://doi.org/10.1093/bioinformatics/btac153.
77. Kanehisa, M., Furumichi, M., Sato, Y., Kawashima, M., and Ishiguro-Watanabe, M. (2023). KEGG for taxonomy-based analysis of pathways and genomes. Nucleic Acids Res. *51*, D587–D592. https://doi.org/10.1093/nar/gkac963.
78. The R Project. (2025). The R Project for Statistical Computing. https://www.r-project.org/.
79. Murray, M.L., Love, S.B., Carpenter, J.R., Hartley, S., Landray, M.J., Mafham, M., Parmar, M.K.B., Pinches, H., and Sydes, M.R.; Healthcare Systems Data for Clinical Trials Collaborative Group (2022). Data provenance and integrity of health-care systems data for clinical trials. Lancet Digit. Health *4*, e567–e568. https://doi.org/10.1016/S2589-7500(22)00122-4.
80. Mason, M.D., Clarke, N.W., James, N.D., Dearnaley, D.P., Spears, M.R., Ritchie, A.W.S., Attard, G., Cross, W., Jones, R.J., Parker, C.C., et al. (2017). Adding Celecoxib With or Without Zoledronic Acid for Hormone-Naive Prostate Cancer: Long-Term Survival Results From an Adaptive, Multiarm, Multistage, Platform, Randomized Controlled Trial. J. Clin. Oncol. *35*, 1530–1541. https://doi.org/10.1200/JCO.2016.69.0677.

STAR★METHODS

KEY RESOURCES TABLE

REAGENT or RESOURCE	SOURCE	IDENTIFIER
Antibodies		
Rabbit Anti-Human Ki-67 antibody	Dako	Cat# A0047; RRID: AB_2314699
Secondary biotinylated universal antibody	Vector lab	Cat# PK-6200; RRID: AB_2336826
PTEN (138G6) Rabbit monoclonal antibody	Cell Signalling Technology	Cat# 9559; RRID: AB_390810
Biological samples		
FFPE tissue	STAMPEDE trial participants	N/A
Chemicals, peptides, and recombinant proteins		
DAB solution	BioGenex	Cat# HK153-5K
Gills 2 Haematoxylin	Merck	Cat# HX43325375
1% Eosin	Sigma	Cat# E4382
Acetic acid	Fisher	Cat# A/0400/PB17
Xylene solvent	Sigma	Cat# 1330-20-7
Ethyl Alcohol 200 Prof	Pharmco by Greenfield Global	Cat# 64-17-5
Critical commercial assays		
RNAeasy FFPE	Qiagen	Cat# 73504
Ovation FFPE	Tecon	Cat# 3400-12
High-density oligonucleotide arrays Affymetrix Human Exon 1.0 ST (HuEx 1.0 ST)	ThermoFisher	Cat# 900651
Roche Ventana BenchMark ULTRA IHC/ISH System	Roche Tissue Diagnostics	Roche Ventana BenchMark ULTRA IHC/ISH System (RRID:SCR_02550)
Hamamatsu NanoZoomer-SQ Digital slide scanner	Hamamatsu Photonics K.K.	Hamamatsu NanoZoomer-SQ Digital slide scanner (RRID:SCR_023763)
Epredia™ SuperFrost Plus™ Adhesion slides	Fisher	Cat# J1800AMNZ
Deposited data		
Gene expression data	NCBI Gene Expression Omnibus	GEO Series accession number GSE: GSE224644
Software and algorithms		
PathwAX II	NA	https://pathwax.sbc.su.se
Decipher GRID	Veracyte, Inc	V3.1
R (v4.3.0)	CRAN	N/A
Survival v3.5.8	CRAN	https://doi.org/10.32614/CRAN.package.survival
mice v3.16.0	CRAN	https://doi.org/10.32614/CRAN.package.mice
survRM2 v1.0.4	CRAN	https://doi.org/10.32614/CRAN.package.survRM2
Hmisc v5.1.2	CRAN	https://doi.org/10.32614/CRAN.package.Hmisc
ggplot2 v3.5.1	CRAN	https://doi.org/10.32614/CRAN.package.ggplot2
KMunicate v0.2.5	CRAN	https://doi.org/10.32614/CRAN.package.KMunicate
affy package in R	Bioconductor	https://www.bioconductor.org/packages/release/bioc/html/affy.html
limma package in R	Bioconductor	https://www.bioconductor.org/packages/release/bioc/html/limma.html
KEGG database	Japan Human Genome Project	https://www.genome.jp/kegg/kegg1.html
Hallmarks of Cancer	Broad Molecular Signatures Database	https://www.gsea-msigdb.org/gsea/msigdb/index.jsp

(*Continued on next page*)

Continued		
REAGENT or RESOURCE	SOURCE	IDENTIFIER
Biomart v2.42.1	Bioconductor	https://bioconductor.org/packages/release/bioc/html/biomaRt.html
pSVA	Bioconductor	https://bioconductor.org/packages/release/bioc/html/sva.html
Other		
Civil Registrations of Death	NHS England	N/A
STAMPEDE trial clinical data	MRC CTU	Linked clinical data is available upon request and after pseudonymization following approval by the MRC CTU at the UCL data access committee
CHAARTED trial clinical data	ECOG-ACRIN	https://www.annalsofoncology.org/article/S0923-7534(21)02050-0/fulltext

EXPERIMENTAL MODEL AND STUDY PARTICIPANT DETAILS

All study participants were male patients (sex assigned at birth), diagnosed with prostate adenocarcinoma.

STAMPEDE trial cohort

Patients were randomized in the STAMPEDE platform protocol (Medical Research Council PR08, ClinicalTrials.gov: NCT00268476, EUDRACT: 2004-000193-31, ISRCTN: ISRCTN78818544)[10,19] sponsored by University College London (UCL). Briefly, patients had prostate adenocarcinoma and were eligible if they had metastatic disease confirmed on conventional whole-body computed tomography and/or technetium bone scans or localized, high-risk disease that was node positive or, if node negative, had at least two of tumor stage category T3/4, PSA $\geq$40ng/ml, Gleason score 8-10. Serum PSA prior to hormone therapy was obtained up to 6 months before randomization. Patient age, World Health Organisation (WHO) performance status, tumor stage (T1-T4), locally-assigned Gleason score, pelvic lymph node negative versus positive, non-metastatic versus metastatic and date of start of ADT (anti-androgens, luteinising hormone releasing hormone agonists or antagonists) were recorded by clinical sites on STAMPEDE case report forms at the time of randomization. Patients were prospectively stratified by pelvic node status and the presence of distant metastases on conventional imaging. Metastatic volume was classified, using scans centrally retrieved after completion of randomization into high (or low) volume based on the presence of visceral metastases or $\geq$4 bone metastases with $\geq$1 outside the vertebral bodies or pelvis.[11,67] Full clinical characteristics are provided in Table S1. Ethnicity data was not collected in the STAMPEDE trials. Date of biopsy was obtained from histopathology reports obtained at time of tissue retrieval. Date of start of ADT was obtained from the STAMPEDE case report forms completed at time of randomization. All patients signed informed consent to participate in the STAMPEDE trials and for use of their tissue for research and data linkage to ascertain long-term survival status (REC04/MRE07/35). Core biopsies from localized tumors (NCCN risk at diagnosis: 29% low, 60% intermediate and 10% high; 42% after prostatectomy) processed by Veracyte for commercial testing and included in the Decipher Genomics Resource for Intelligent Discovery (GRID, ClinicalTrials.gov: NCT02609269) were used for optimization of signatures and for comparison with STAMPEDE tumors.

CHAARTED trial cohort

The CHAARTED trial (ClinicalTrials.gov: NCT00309985) randomized patients with metastatic prostate adenocarcinoma to ADT or ADT and docetaxel. It was designed and coordinated by the Eastern Cooperative Oncology Group-ACRIN Cancer Research Group (ECOG-ACRIN) and was approved by the institutional review board at each participating institution. The ECOG-ACRIN Statistical Center collected the data and was the data coordinating center. Patients consented to use of their samples and Institutional Review Board (Dana-Farber Cancer Institute) approval was obtained. Transcriptional profiling of the CHAARTED biomarker cohort (n=160) has been previously published.[20] The median age of the CHAARTED biomarker cohort was 63 years (range 39-90 years), 14 (8.8%) patients were described as African descent and 146 (91.2%) patients described as being of a different or unknown race.

METHOD DETAILS

Study design

Prior to testing association with clinical outcome data from the abiraterone trial, a statistical analysis plan was defined (v1.0, locked and signed 21st March 2022). This selected a single signature for primary survival analysis, Decipher,[40] and four signatures for primary predictive analyses (i.e., interaction of signature with treatment effect), namely AR-A_Spratt,[29] PAM50,[21] PSC[22] and Decipher[22,40] (in this order using a closed hierarchical test). For the docetaxel trials analysis, a separate analysis plan was written, informed by the analyses of the abiraterone STAMPEDE trial and the CHAARTED trial (v1.0, locked and signed 3rd July 2023). This selected three

signatures (Decipher, PAM50 and PSC) for primary survival and predictive testing. Both statistical analysis plans were revised (v2.0 signed 5th March 2024 and an update to the abiraterone statistical analysis plan signed 20th March 2024) to pool prognostic analyses across both trials and use overall survival as the sole primary end-point, enabled by the greater statistical power afforded by linkage to civil registrations of death in February 2024. Transcriptome signatures for predictive testing, as pre-defined in our statistical analysis plans, were selected based on data generated from the CHAARTED biomarker cohort which served as our pilot set (n=160).

Analyses were overseen by the STAMPEDE Biological Research Group and defined in the STRATOSPHERE (STratification for RAtional Treatment-Oncomarker Pairings of STAMPEDE patients starting long-term Hormone treatment) consortium protocol for molecular studies on tumors collected from patients treated in the STAMPEDE trial, approved by an independent Research Ethics Committee (REC18/LO/1235) and the STAMPEDE Trial Management Group and Trial Steering Committee. The framework for analyses was two-stage: feasibility analyses for genome, methylome or transcriptome on a pilot cohort of 50-100 patients (Stage I) followed by extension of the approach with the highest success rate (Stage II). The success rate for expression array analysis was 92%, so this was selected as the preferred approach (n=109 core biopsies from 50 control arm patients, presented at ASCO Genitourinary Cancers Symposium, February 2020, San Francisco USA, abstract #153). Genomic analyses are described elsewhere.[68]

Sample retrieval and processing

Tissue blocks were retrieved from STAMPEDE trial sites upon request by the Medical Research Council Clinical Trials Unit at UCL and centralized at the Wales Cancer Biobank (Biobank Cancer Cymru) where all identifying details were removed. Pseudo-anonymized tissue blocks were transferred to the UCL Cancer Institute (London, UK) for processing. Laboratory researchers had no access to clinical data other than pseudo-anonymized local pathology reports. Sample type was recorded and central pathology review of freshly-cut hematoxylin and eosin (H&E) slides was performed (L. Mendes, D.M.B.). The tumor block containing the index core (selected using the following hierarchy: the highest primary Gleason score, the highest secondary Gleason score, the longest tumor length) was then sectioned onto 10 to 15 glass slides. Areas with at least 30% cancer purity were macrodissected and the tissue used for RNA extraction. When fewer than the target number of slides were obtained prior to block exhaustion, analyses were prioritized as follows: extraction of RNA; immunostaining in the order of Ki-67, followed by PTEN. Transurethral resections of the prostate and prostatectomies were not evaluated for immunohistochemistry markers; samples with technical artefacts were excluded.

Ki-67 staining and assessment

Ki-67 immunohistochemistry assay used the MIB-1 antibody (Dako) which was previously-validated[69,70] at two laboratories (Barts Cancer Institute, UCL Cancer Institute). Assessment was done by two trained uropathologists (L. Mendes, D.M.B.) who generated a semi-quantitative score with cases categorized by 5% increases. For analysis, numerical values were assigned to bins as follows: 0 for '$\leq$0.01'; 0.025 for '>0.01–<0.5'; 0.05 for '0.05–<10'; 0.10 for '$\geq$10–<15'; thereafter continuing in 5% increments using the value of the lower bound of scoring intervals.

PTEN staining and assessment

PTEN immunostaining was performed at the Johns Hopkins School of Medicine using previously described protocols optimized on the Ventana Benchmark immunostaining system.[49] The PTEN (Cell Signaling Technology, Clone D4.3 XP) antibody was utilized with the Optiview secondary detection kit. Two trained uropathologists blindly scored for PTEN using a validated and previously described scoring system. In brief, PTEN was scored as lost if some (heterogeneous loss) or all (homogeneous loss) tumor glands showed absence of protein expression compared to surrounding benign glands, stroma, nerves and endothelial cells, which provided an internal positive control.[49]

Transcriptome expression data generation

Between 6th March 2019 and 10th March 2022 (abiraterone trial) and between October 2022 and October 2023 (docetaxel trials), RNA was analyzed for expression of 1.4 million genome-wide features (including all known genes and most of the non-coding RNAs) in the Veracyte CLIA lab (San Diego, CA, USA) using high-density oligonucleotide arrays (Affymetrix Human Exon 1.0 ST, ThermoFisher, Santa Clara, CA, USA). Expression data were quality controlled by visualizing density and relative expression plots before and after background correction and quantile normalization using the affy package in R.[71] Multi-dimensional scaling plots were used to inspect for possible batch effects and corrected using pSVA if needed. Data normalization was performed using Single Channel Array Normalization, where each sample was compared to itself using control probes from the array.[72] The Decipher GRID, including expression profiles of 80,071 cancers from prospective clinical use of the Decipher test and retrospective studies of institutional cohorts, was used to check the clustering solution and its analytical validity. Patients' data were de-identified in accordance with the Safe Harbor method described in the HIPAA Privacy Rule 45 CFR 164.514 and prior to analysis (Veracyte, Inc., San Diego, CA). For the CHAARTED biomarker cohort, RNA data used to generate signature scores was produced using the same array technology at an earlier and independent timepoint in a different batch from STAMPEDE, as described previously.[20]

QUANTIFICATION AND STATISTICAL ANALYSIS

Generation of transcriptome signature scores

Normalized expression values for 46,050 genes were obtained and used to generate signature scores. Signature names are from the original publication or if no name was assigned, the nomenclature adopted was the biological pathway the signature was developed to represent with suffix of the consortium or first author name. Prior to analysis of the STAMPEDE dataset, each signature was assigned to one of twelve biological categories based on the process or experimental aims that led to its discovery, namely prostate cancer subtyping, measures of signaling activity of the androgen receptor and related steroid receptors, chromatin remodeling, radiosensitivity, prognostic in localized disease and hallmarks of cancer, namely genome instability, metabolism, immune activity, angiogenesis and other features of the microenvironment, DNA repair, oncogenic pathways and cellular plasticity. Spearman correlation coefficients were calculated between signatures using R (v4.3.0). PAM50 was split into three classes: basal, luminal A and luminal B. PSC was split into four classes: Basal Immune, Basal Neuroendocrine-like, Luminal Proliferating and Luminal Differentiated. Primary analyses of PSC and exploratory analyses on PAM50 were on quantile-matched scores, obtained by matching the expression data of the STAMPEDE biomarker analysis cohort to the subset of the Decipher GRID classed as NCCN very high-risk (1,412 samples) and then assigning PSC and PAM50 subtypes based on the matched expression data. Two-way analyses of variance were used to assess differences in score distributions adjusted for initiation of ADT prior to biopsy.

Pathway enrichment analysis

Differential gene expression analysis was carried out using the lmFit and eBayes functions from the limma package in R. The Spearman rank correlation coefficient between signature score and all other genes was calculated in the whole cohort and also in metastatic and non-metastatic cancers separately. Genes which had $q<0.05$ and absolute Spearman rank correlation coefficient >0.3 or $<=0.3$ were included in pathway annotation (only signatures for which more than one gene met this threshold were included). The Benjamini-Hochberg correction[73] was applied to correct the p values for multiple testing. The R package Biomart v2.42.1[74,75] was used to map gene symbols to ENSG. PathwAX II[76] was used alongside the KEGG database[77] to annotate pathways.

Statistical clinical outcome analyses

Analyses were performed using R (v4.3.0)[78] by unblinded clinical trial unit statisticians (P.D.-M., L. Murphy, C.B.) according to prespecified statistical analysis plans. The primary outcome was overall survival (time from randomization to death from any cause). This was obtained from case report forms based on data from the final trial locks (STAMPEDE docetaxel trials on the 13th July 2018, abiraterone trial on the 3rd July 2022 and CHAARTED trial on the 23rd April 2016) and additionally STAMPEDE participants in England were linked to civil registrations of death in February 2024 as described previously.[79] STAMPEDE patients in Scotland and Northern Ireland were not linked to civil registrations of deaths but censored on the last date known to be alive from the trial case report forms. The secondary outcome measure, tested when there was a significant association with overall survival, was metastatic progression-free survival (time from randomization to first of: distant metastases progression, skeletal-related event confirmed as disease progression, or death classified as due to prostate cancer).

To estimate the association with survival of a signature, multivariable Cox proportional hazard models were used with covariate adjustment for treatment allocation and baseline characteristics, of which six were used as randomization minimization factors: age (continuous), WHO performance status (0; 1-2), regular aspirin or non-steroidal anti-inflammatory drugs use (included as a randomization minimization factor when STAMPEDE was testing celecoxib[80]), serum PSA prior to start of ADT (ng/ml, log-transformed), Gleason score assessed by local pathologist (<=6; 7; >=8), nodal stage and tumor stage (T0-T2; T3; T4) and in metastatic cases, metastatic volume categorization (low-volume versus high-volume disease as per CHAARTED trial definition[20]). Point and interval hazard ratios provided a measure for the association of a signature with hazard of death. Statistical significance was assessed using partial likelihood ratio tests with a Bonferroni-corrected p value threshold of 0.05/60, equivalent to $8.3.10^{-4}$. For continuous signatures, hazard ratios were calculated to the power of 1 standard deviation (estimated from the signature in the full biomarker cohort, n=1523) to produce standardized hazard ratios (sdHR), measuring the effect of a 1 standard deviation increase in the signature on its original scale. This standardization allowed inter-signature comparisons by overcoming differences in scale. We also dichotomized all continuous signatures by the median score in the metastatic cohort for association with clinical endpoints.

To estimate the predictive effect of biomarker subgroups (Decipher>0.80,[40] PAM50,[21] PSC,[22] AR-A_Spratt,[29] PTEN_loss_Liu>0.30[25]), interaction effects between treatment allocation and signature scores or classifier subgroups were added to the aforementioned prognostic models. We pre-specified dichotomization by the median Decipher score in the metastatic cohort to categorize tumors as either Decipher ‘‘high’’ or ‘‘lower’’. We also dichotomized tumors based on PTEN_loss_Liu score due to the bimodal distribution of the signature. Subgroup-specific hazard ratios for the treatment effect of docetaxel or abiraterone were compared to assess the clinical significance of the predictive effect. Partial likelihood ratio tests were used to assess statistical significance. Deviations from the proportional hazard assumption in the prognostic or predictive effect of interest were identified using Grambsch-Therneau tests with log-transformed time, and assessed further by examining cumulative hazard curves. Restricted mean survival time difference at 5 years was calculated to confirm clinical significance and planned as the main treatment effect measure when non-proportional hazards were observed. The difference in 5-year restricted mean survival time between categories was estimated

using a bias-corrected bootstrap and considered positive if there was an absolute difference in patients with a score greater than the median compared to patients with a score lower than the median.

Nodal stage, tumor stage, and metastatic volume missingness was associated with prognosis, pre-ADT serum PSA, and initiation of ADT prior to biopsy, and therefore assumed to be missing at random (MAR). Multiple imputation with chained equations (MICE) was therefore used to impute all three variables in non-metastatic and metastatic disease separately. Baseline covariates, presence of metastases by site at randomization (bone, lung, liver, node), initiation of ADT prior to biopsy, Nelson-Aalen estimates of cumulative hazard, death status, Decipher score,[40] PAM50 class,[21] PSC class,[22] and AR-A_Spratt[29] were used in the imputation model.

Two sensitivity analyses were performed and are included in Tables S7, S8 and S11. First, estimates from complete case analyses are reported alongside MICE estimates. Second, analyses were repeated in patients with tissue collected before initiation of ADT.

As pre-specified in our statistical analysis plan, exploratory discoveries of interest were validated in the CHAARTED clinical trial. The association between the PTEN inactivity score and overall survival in the CHAARTED biomarker cohort was performed once all primary objectives had been met in the STAMPEDE trial cohort. To estimate the association with survival of PTEN inactivity, multivariable Cox proportional hazard models were used with covariate adjustment for age, WHO performance status, prior local treatment in relapsed disease, and metastatic volume.

ADDITIONAL RESOURCES

STAMPEDE trial website: https://www.stampedetrial.org/.

STAMPEDE trial registration, ClinicalTrials.gov: NCT00268476, registered on December 22, 2005. EudraCT: 2004-000193-31, registered on October 4, 2004.

CHAARTED trial registration, ClinicalTrials.gov: NCT00309985.

Statistical analyses plan: https://doi.org/10.5281/zenodo.16327659.

CellPress
OPEN ACCESS

Supplemental figures

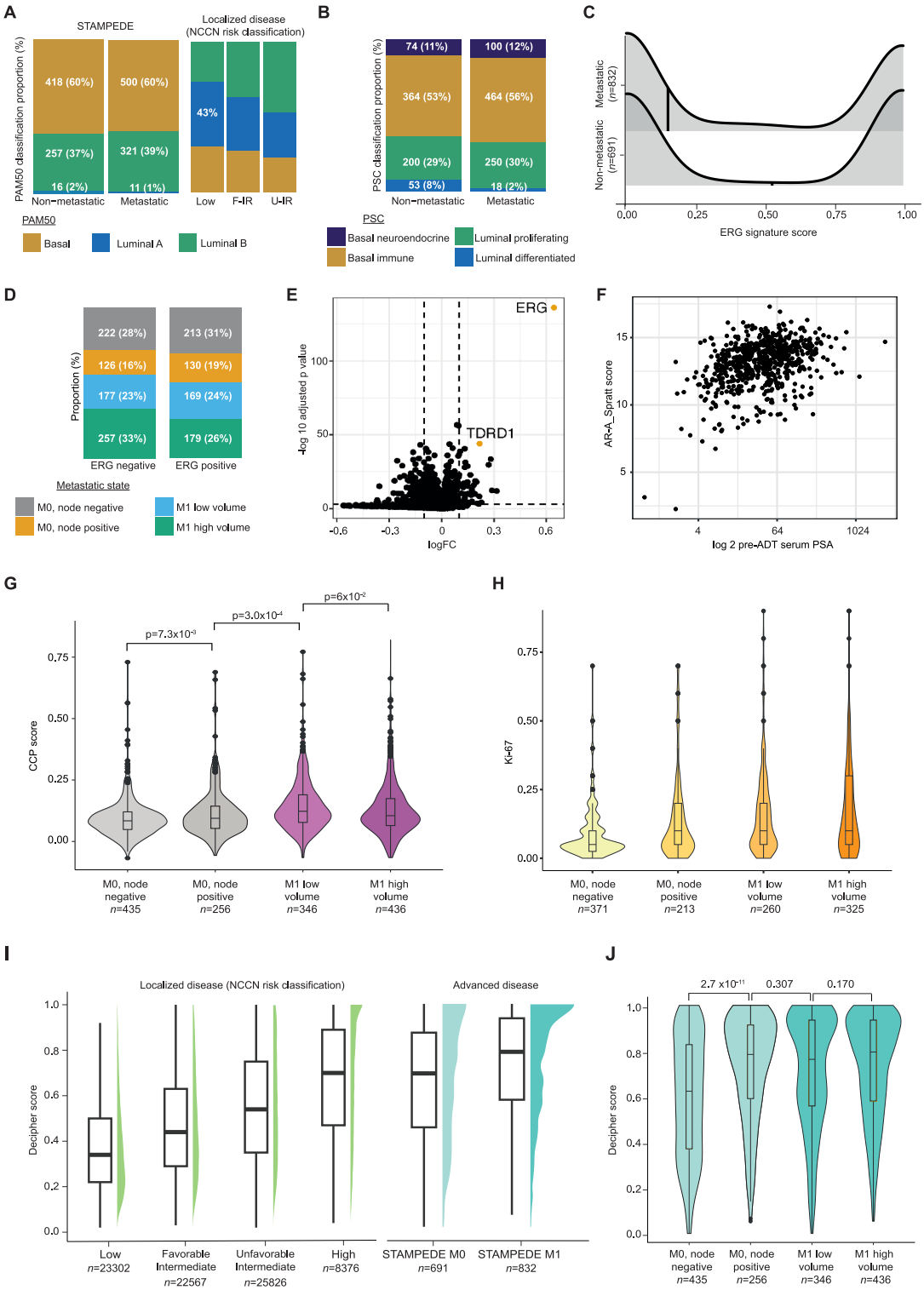

(legend on next page)

Figure S1. Distributions of selected classifier subgroups in STAMPEDE prostate tumors, related to Figure 3

(A) Stacked bar chart demonstrating the proportion of PAM50 subtypes in STAMPEDE prostate tumors (left) split by metastatic status and localized prostate cancer (right) split by NCCN low risk, favorable intermediate (F-IR), and unfavorable intermediate risk (U-IR).

(B) Stacked bar chart demonstrating the proportion of PSC basal-luminal subtypes in STAMPEDE prostate tumors split by metastatic status.

(C) Density plot showing bimodal distribution of ERG signature scores in non-metastatic and metastatic STAMPEDE prostate tumors. Vertical lines represent the median ERG score in each cohort.

(D) Stacked bar chart demonstrating the proportion of ERG-positive and -negative STAMPEDE prostate tumors across metastatic state.

(E) Differential gene expression analyses of ERG-fusion-positive versus -negative tumors. *ERG* and *TDR1* genes highlighted with yellow dots.

(F) Scatterplot demonstrating the association between AR-A_Spratt signature score and pre-ADT serum PSA in STAMPEDE non-metastatic patients (n = 652; patients that initiated ADT prior to biopsy excluded).

(G) Box-violin plot shows distribution by metastatic state of CCP score, including p values from F test acquired from two-way analyses of variance (ANOVAs).

(H) Box-violin plot shows distribution by metastatic state of Ki-67 immunohistochemistry score.

(I and J) Box-and-whisker and density plots showing the distribution of Decipher scores for (I) localized prostate cancer split by NCCN risk category and STAMPEDE prostate tumors split by metastatic status and (J) for STAMPEDE prostate tumors split by nodal status and metastatic volume, including p values arising from F tests from ANOVAs.

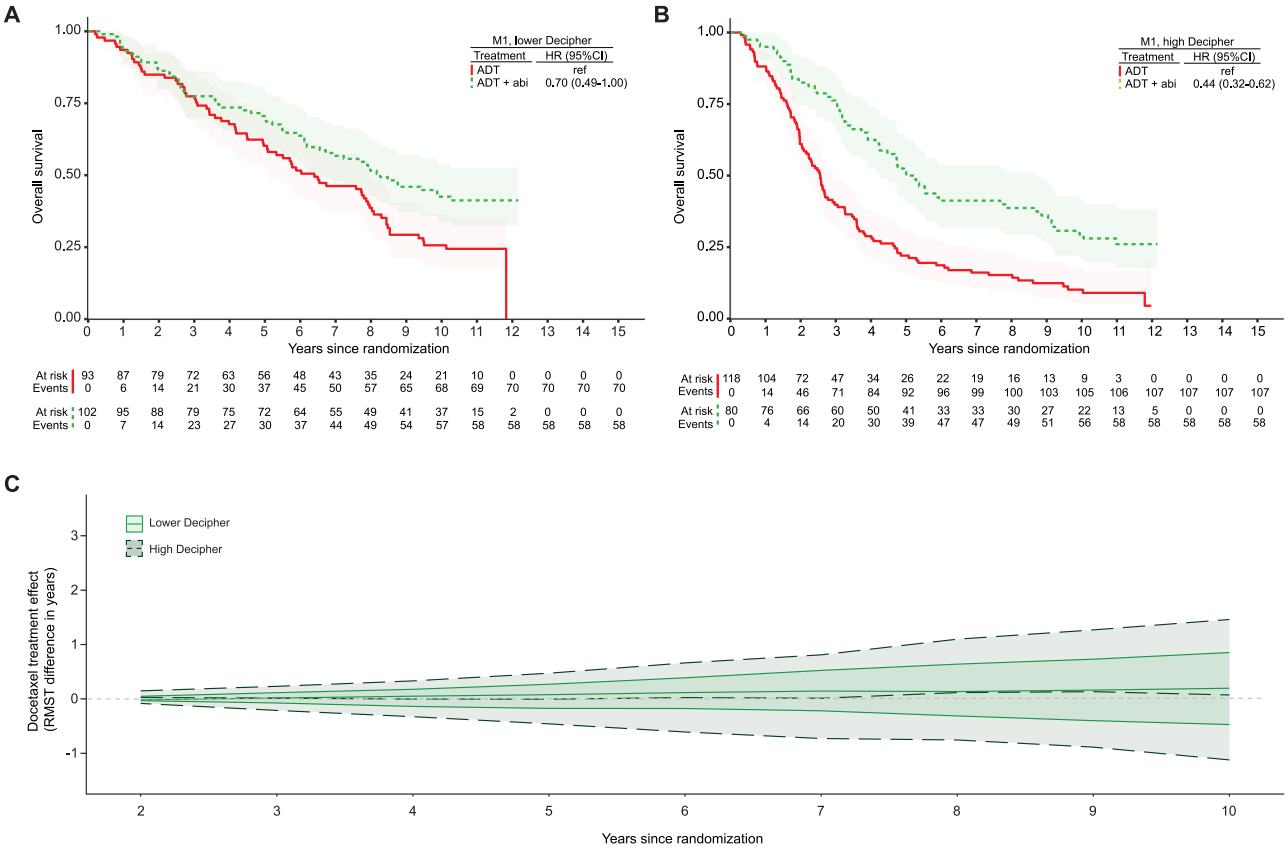

Figure S2. Abiraterone efficacy in metastatic disease and docetaxel efficacy in non-metastatic disease, split by Decipher classifier, related to Figure 5

(A and B) Kaplan-Meier plots of overall survival in patients with metastatic disease in the STAMPEDE abiraterone trial, allocated to either ADT (red solid line) or ADT and abiraterone (green dashed line), split by pre-specified lower (A) versus (B) high Decipher classifier. HRs and 95% CIs are included as insets. Shaded areas represent 95% CIs.

(C) Restricted mean survival time (RMST) analyses show survival differences (dashed gray line marks 0 difference) over time by treatment allocation for patients with non-metastatic disease split by high Decipher (dark green, dashed line) or lower Decipher classifier (light green, solid line) in the docetaxel trials. HRs and 95% CIs are included as insets. Shaded areas represent 95% CIs.

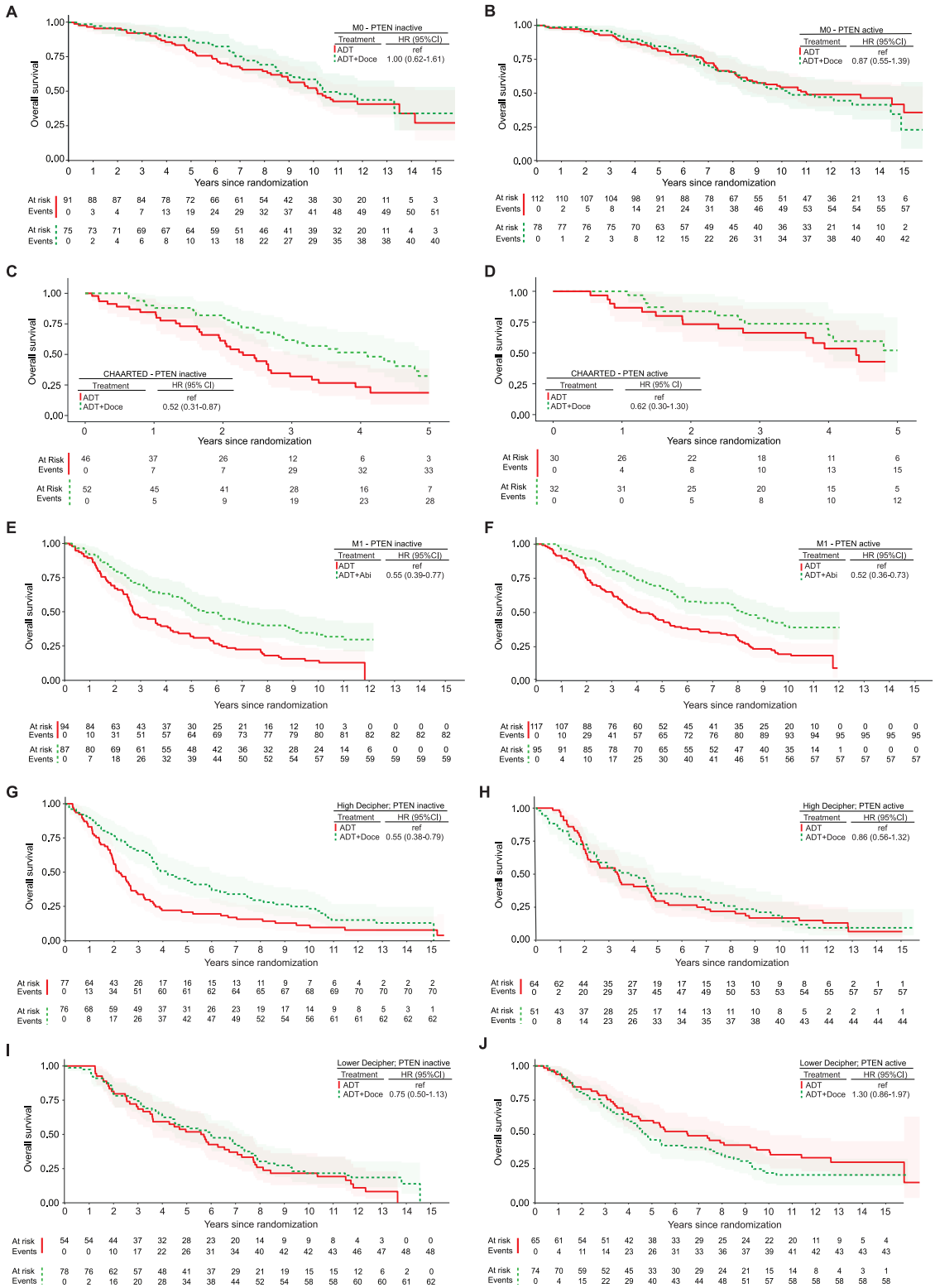

Figure S3. Docetaxel and abiraterone efficacy split by PTEN activity, related to Figures 6 and 7

(A and B) Kaplan-Meier plots of overall survival in patients with non-metastatic disease in the STAMPEDE docetaxel trials allocated to either ADT (red solid line) or ADT with docetaxel ± zoledronic acid (green dashed line) split by (A) PTEN-inactive or (B) PTEN-active disease.

(legend continued on next page)

(C and D) Kaplan-Meier plots of overall survival in patients with metastatic disease in the CHAARTED docetaxel trial allocated to either ADT (red solid line) or ADT with docetaxel (green dashed line) split by (C) PTEN-inactive or (D) PTEN-active disease.
(E and F) Kaplan-Meier plots of overall survival in patients with metastatic disease in the STAMPEDE abiraterone trial allocated to either ADT (red solid line) or ADT with abiraterone (green dashed line) split bya (E) PTEN-inactive or (F) PTEN-active disease.
(G–J) Kaplan-Meier plots of overall survival in patients with metastatic disease in the STAMPEDE docetaxel trials allocated to either ADT (red solid line) or ADT with docetaxel ± zoledronic acid (green dashed line) split by (G) high Decipher; PTEN inactive or (H) high Decipher; PTEN active or (I) lower Decipher; PTEN inactive or (J) lower Decipher; PTEN active. HRs and 95% CIs are included as insets. Shaded areas represent 95% confidence intervals.